

AD-A120 531

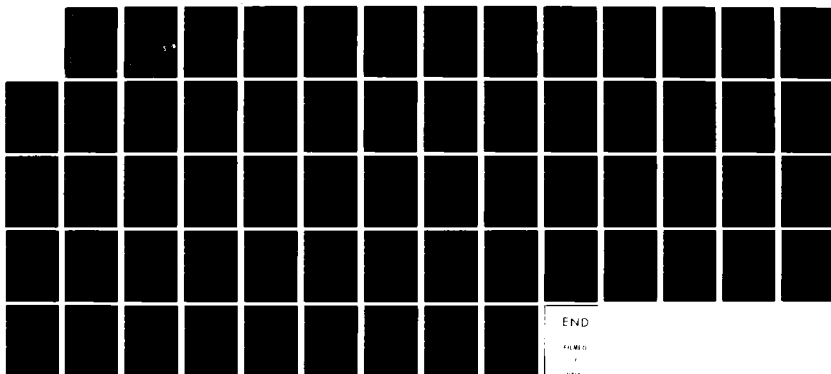
CROSSED MOLECULAR BEAM STUDY OF THE REACTIONS OF OXYGEN
AND FLUORINE ATOMS(U) CALIFORNIA UNIV BERKELEY DEPT OF
CHEMISTRY Y T LEE 21 SEP 82 N00014-75-C-0671

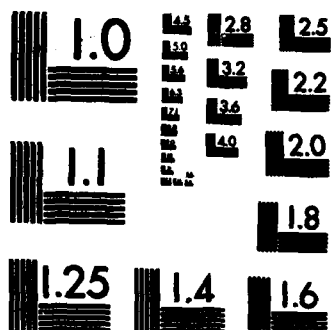
1/1

UNCLASSIFIED

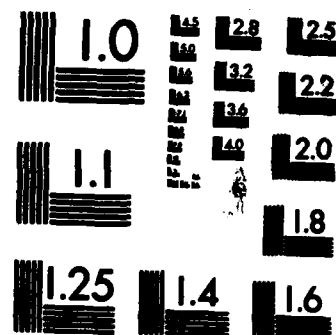
F/G 20/5

NL

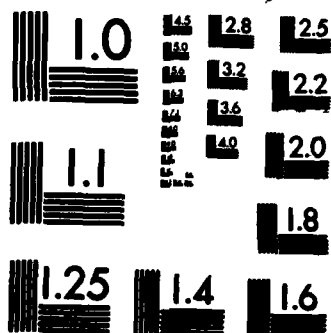




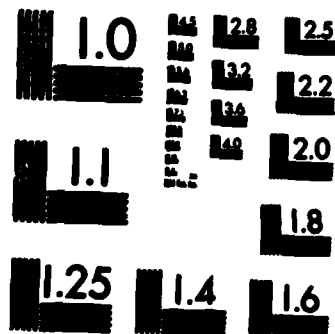
MICROCOPY RESOLUTION TEST CHART
NATIONAL BUREAU OF STANDARDS-1963-A



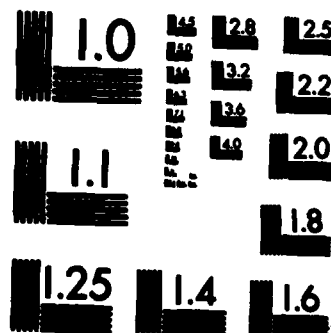
MICROCOPY RESOLUTION TEST CHART
NATIONAL BUREAU OF STANDARDS-1963-A



MICROCOPY RESOLUTION TEST CHART
NATIONAL BUREAU OF STANDARDS-1963-A



MICROCOPY RESOLUTION TEST CHART
NATIONAL BUREAU OF STANDARDS-1963-A



MICROCOPY RESOLUTION TEST CHART
NATIONAL BUREAU OF STANDARDS-1963-A

UNCLASSIFIED

12

SECURITY CLASSIFICATION OF THIS PAGE (When Data Entered)

REPORT DOCUMENTATION PAGE		READ INSTRUCTIONS BEFORE COMPLETING FORM
1. REPORT NUMBER NR 092-545/9/82	2. GOVT ACCESSION NO. AD-A120 531	3. RECIPIENT'S CATALOG NUMBER
4. TITLE (and Subtitle) Crossed Molecular Beam Study of the Reactions of Oxygen and Fluorine Atoms		5. TYPE OF REPORT & PERIOD COVERED Annual Report 4/1/81-8/30/82
		6. PERFORMING ORG. REPORT NUMBER
7. AUTHOR(s) Yuan T. Lee		8. CONTRACT OR GRANT NUMBER(s) N00014-75-C-0671 NR 092-545
9. PERFORMING ORGANIZATION NAME AND ADDRESS Professor Y. T. Lee Department of Chemistry, University of Calif. Berkeley, California 94720		10. PROGRAM ELEMENT, PROJECT, TASK AREA & WORK UNIT NUMBERS
11. CONTROLLING OFFICE NAME AND ADDRESS Dr. Richard Miller, Office of Naval Research Department of the Navy, Code 432 800 N. Quincy St., Arlington, VA 22217		12. REPORT DATE September 21, 1982
14. MONITORING AGENCY NAME & ADDRESS (if different from Controlling Office) Office of Naval Research Resident Representative University of California 239 Campbell Hall Berkeley, California 94720		13. NUMBER OF PAGES 62
16. DISTRIBUTION STATEMENT (of this Report) Unlimited		15. SECURITY CLASS. (of this report) UNCLASSIFIED
		15a. DECLASSIFICATION/DOWNGRADING SCHEDULE
17. DISTRIBUTION STATEMENT (of the abstract entered in Block 20, if different from Report)		
18. SUPPLEMENTARY NOTES		
19. KEY WORDS (Continue on reverse side if necessary and identify by block number) Ethyl Vinyl Ether Toluene Diethyl Ether Photodissociation Nitromethane Unimolecular Decomposition Nitroethane Laser Chemistry Cycloheptatriene		
20. ABSTRACT (Continue on reverse side if necessary and identify by block number) → Using the method of photofragmentation translational spectroscopy, photodissociation of ethyl-vinyl ether, diethyl ether, nitromethane, nitroethane, and cycloheptatriene have been investigated. For concerted reactions involving the formation of a cyclic transition state, a large fraction of the exit potential energy barriers appear as translational.		

AD A120531

DTIC FILE COPY

DTIC
ELECTE
S OCT 20 1982
H D

DD FORM 1473
1 JAN 73EDITION OF 1 NOV 65 IS OBSOLETE
S/N 0102-LP-014-6601

SECURITY CLASSIFICATION OF THIS PAGE (When Data Entered)

82 10 19 034

Annual Report on Contract Research Entitled

**CROSSED MOLECULAR BEAM STUDY OF THE
REACTIONS OF OXYGEN AND FLUORINE ATOMS**

**Prepared for the
Office of Naval Research
Department of the Navy**

**By
Yuan T. Lee
Professor of Chemistry
University of California
Berkeley, California 947820**

Period Covered: April 1, 1981 to August 30, 1982

Technical Report No. NR 092-545/9/82

Contract No. N00014-75-C-0671

September 21, 1982

INTRODUCTION

Since 1980, the direction of our program has changed to emphasize the decomposition of polyatomic molecules related to energetic materials, although we have retained the title of "Crossed Molecular Beam Study of the Reactions of Oxygen and Fluorine Atoms." Our research during this period has yielded results which prove the value of the molecular beam photofragmentation spectroscopy method for the study of energetic materials decomposition. Several laser excitation methods have been used to probe the reaction dynamics and the mechanisms of molecular decomposition. Our results have uncovered intriguing features of the dynamics when vastly different reaction pathways compete. The high translational energy found in the products of some of these reactions suggest important areas for further study, including the effects of high energy collisions for inducing molecular decomposition. Four systems which will be summarized here are listed below.

1. Competitive decay channels in multiple photon excited ethyl vinyl ether.
2. Mechanism for decomposition of laser excited diethyl ether.
3. Photofragmentation of CH_3NO_2 and $\text{C}_2\text{H}_5\text{NO}_2$.
4. Unimolecular decay of toluene after isomerization of laser excited cycloheptatriene.

1. COMPETING DISSOCIATION CHANNELS IN THE INFRARED MULTIPHOTON DECOMPOSITION OF ETHYL VINYL ETHER

F. Huisken,^a D. Krajnovich,^b Z. Zhang,^c Y. R. Shen^d and Y. T. Lee^{b,e}

Infrared multiphoton decomposition of ethyl vinyl ether (EVE) has been investigated by the crossed laser-molecular beam technique. Competition is observed between the two lowest-energy dissociation channels: (1) $\text{EVE} \rightarrow \text{CH}_3\text{CHO} + \text{C}_2\text{H}_4$, and (2) $\text{EVE} \rightarrow \text{CH}_2\text{CHO} + \text{C}_2\text{H}_5$. Center-of-mass product translational energy distributions were obtained for both dissociation channels. The products of reactions (1) and (2) are formed with mean translational energies of 31 kcal/mole and 5 kcal/mole, respectively. The branching ratio shifts dramatically in favor of the higher energy radical producing channel as the laser intensity and energy fluence are increased, in agreement with the qualitative predictions of statistical unimolecular rate theory.



Accession For	
DTIC GRAAI	<input checked="" type="checkbox"/>
DTIC TAB	<input type="checkbox"/>
Unannounced	<input type="checkbox"/>
Justification	
By	
Distribution/	
Availability Codes	
Dist	Avail and/or Special
A	

I. INTRODUCTION

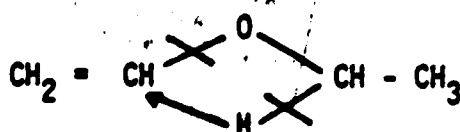
The thermal decomposition of many aliphatic ethers appears to proceed through a concerted rearrangement mechanism in which a hydrogen atom is transferred from one aliphatic group to the other. Wang and Winkler¹ studied the thermal decomposition of ethyl vinyl ether (EVE) in a static system in the temperature range 377–448°C. They found that EVE decomposes mainly to give acetaldehyde and ethylene



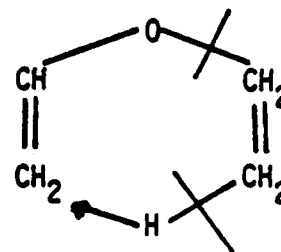
at a rate given by $k_1 = 4 \times 10^{11} \exp(-44000/RT) \text{ sec}^{-1}$. They also found evidence for a minor free radical pathway.

Blades and Murphy² reinvestigated the thermal decomposition of EVE between 497–586°C in a flow system. In an attempt to focus their attention on the intramolecular rearrangement reaction, they employed toluene as a carrier gas to help suppress free radical interference. While they obtained Arrhenius parameters³ for rxn. (1) in satisfactory agreement with those of Wang and Winkler, they still were unable to completely eliminate the secondary free radical reactions.

Two types of cyclic intermediate have been proposed for rxn. (1):



(I)



(II)

Wang and Winkler favored (I) on energetic grounds, while Blades and Murphy preferred (II) on the basis of entropy of activation arguments. If (I) is the correct intermediate, ethylene and acetaldehyde are formed from vinyl and ethyl groups, respectively. If (II) is correct, the opposite is true. Molera et al.³ settled this issue using radioactive tracers. They labeled the ethyl group of EVE with carbon-14. After pyrolysis, the amounts and specific activities of the products were determined. They found that, at temperatures around 450°C, most (78%) of the carbon-14 label ended up in the ethylene product, suggesting that the rearrangement reaction proceeds through a hexagonal transition state. The remaining ether (22%) decomposed according to secondary free radical processes.

The nature of these radical processes is not so well understood. Some possible EVE dissociation channels are depicted in Fig. 1. The lowest energy free radical pathway is



This agrees with our chemical intuition that, of the two C-O bonds, the one adjacent to the C-C double bond should be stronger. Although previous workers seem to have unanimously assumed that rxn.(2) is the major source of free radicals, direct confirmation is lacking. (The CH_2CHO radical has, however, been detected in the mercury sensitized decomposition of EVE.⁶)

The unimolecular decomposition of EVE has been investigated more recently using the technique of infrared multiphoton absorption in place of thermal heating to vibrationally excite the molecules. Rosenfeld et al.⁷

studied multiphoton dissociation of EVE at pressures between 5 and 440 torr where the reaction is mainly collisional in nature. With an unfocussed laser beam only acetaldehyde and ethylene were observed, but with a focussed beam comparable amounts of ketene, ethane and butane were also formed, indicating competition from free radical processes. Brenner⁸ studied multiphoton dissociation of EVE using laser pulses of different durations (0.2 and 2 μ s) but constant energy fluence. With the 2 μ s pulses only rxn.(1) was observed. With the 0.2 μ s pulses, however, radical processes were found to dominate over rxn.(1). Brenner interpreted these observations as possible evidence of a non-statistical distribution of energy in the molecules prior to reaction.

In the present work, the crossed laser-molecular beam method has been used to study the unimolecular decomposition of EVE under collision-free conditions. Competition between rxns. (1) and (2) is observed. For each reaction, laboratory angular and velocity distributions of the dissociation products were measured and used to determine the center-of-mass (CM) product translational energy distribution. The dependence of the product branching ratio on the laser intensity and energy fluence was also investigated. The results are discussed in the context of a very simple rate equation model, which assumes, for molecules above the dissociation threshold, a competition between the intensity-dependent excitation rate and the rate of statistical unimolecular reaction.

II. EXPERIMENTAL

The experiments were carried out in a molecular beam apparatus which has been described in detail elsewhere.⁹ The molecular beam was formed by bubbling helium through an EVE reservoir maintained at -32°C and expanding the mixture through a 0.1 mm diameter quartz nozzle at a total stagnation pressure of 320 torr (15% EVE/85% He). The nozzle was heated to 300°C to enhance multiphoton absorption and to reduce the concentration of molecular clusters in the beam. The velocity distribution of the EVE beam was determined by time-of-flight (TOF) measurements. The beam had a peak velocity of 1710 m/s whereas the full width at half maximum (FWHM) of the distribution was 21%. The beam was collimated by a skimmer, and, after passing through two pressure reducing differential chambers with suitable skimmer-like apertures, it was crossed by the laser beam. The molecular beam was defined to an angular divergence of $\sim 1.5^{\circ}$.

The IR laser we used was a high repetition rate Gentec DD-250 CO_2 TEA laser. The laser was tuned to 1041.3 cm^{-1} (the P(26) line of the 001-020 vibrational band). EVE has absorption bands at 1048, 1069 and 1081 cm^{-1} , although these are not all due to the same rotational isomer.¹⁰ As in previous experiments, the energy fluence was adjusted by varying the distance between a 25 cm focal length ZnSe lens and the molecular beam.

The dissociation products were detected in the plane of the laser and molecular beams by a rotatable ultra-high vacuum mass spectrometer consisting of an electron bombardment ionizer, quadrupole mass filter, and particle counter. Angular and TOF distributions of the products were measured in the usual way.¹¹ Signal was observed when the quadrupole mass spectrometer was

set to pass the following mass to charge ratios: $m/e = 43, 42, 41, 29, 27, 26, 25, 15$ and 14 . The signal levels at these masses ranged between 0.1 – 0.6 counts/laser pulse (at a detector angle of 20° and a laser energy fluence of 1.8 J/cm^2). No signal was observed at $m/e = 45, 44$ or 30 .

III. RESULTS AND ANALYSIS

A. Identification of Primary Products

Figure 2 shows the TOF distributions for $m/e = 43$, 42 and 26 obtained at a laboratory deflection angle of 20° . The laser energy fluence was approximately 1.8 J/cm^2 . Without any detailed analysis we can already state the following. The TOF spectra of $m/e = 43$ and $m/e = 42$ look quite different and peak at different positions implying that they cannot stem from the same product. Since the masses are both greater than half that of EVE ($m = 72$), we can conclude that we are dealing with at least two different dissociation channels.

The peak of the $m/e = 42$ TOF spectrum, when converted to velocity, is only a little faster than the EVE beam velocity, indicating that the average CM translational energy of this product is very small. This product probably results from a simple radical split. The product measured at $m/e = 43$ is much faster, suggesting the presence of a large exit potential energy barrier in this dissociation channel. Such barriers are characteristic of concerted chemical reactions in which bonds are broken and formed simultaneously. The shoulder on the fast side of the $m/e = 42$ spectrum is due to a contribution from the same product which also generates the $m/e = 43$ spectrum. The TOF distribution for $m/e = 26$ shows two partially resolved peaks, again reflecting the existence of two dissociation channels. The slow peak on the right hand side corresponds to a product moving slightly faster than the product responsible for the $m/e = 42$ spectrum and the fast peak on the left hand side corresponds to a product which is even faster than that detected at $m/e = 43$. Thus, the two peaks in the $m/e = 26$ spectrum appear to correspond to the light counterparts of the heavy products monitored at $m/e = 43$ and $m/e = 42$.

The most reasonable interpretation of the data, consistent with the energetics and the thermal decomposition results, is that the $m/e = 43$ signal is due to acetaldehyde ($m = 44$) produced in rxn. (1), and that the $m/e = 42$ signal is due to CH_2CHO ($m = 43$) produced in rxn. (2). Then, in the $m/e = 26$ TOF spectrum, we see contributions from ethylene ($m = 28$) and C_2H_5 ($m = 29$). There is one problem with this identification: why are the parent ions of acetaldehyde and CH_2CHO not detected at $m/e = 44$ and 43, respectively. In the case of the CH_2CHO radical, our failure to observe the parent ion is not too surprising. In a recent crossed molecular beam study¹² of the reaction $\text{O} + \text{C}_2\text{H}_4 \rightarrow \text{CH}_2\text{CHO} + \text{H}$, it was found that the CH_2CHO radicals produced about twenty times more $\text{C}_2\text{H}_2\text{O}^+$ ions than parent ions in the electron bombardment ionizer. More disturbing is our failure to observe the parent ion of acetaldehyde. Despite repeated efforts, we were unable to detect any signal at $m/e = 44$, even though the mass spectral tables¹³ indicate that acetaldehyde produces comparable amounts of mass 44 and 43 ions. Although our experimental sensitivity is poorer at mass 44 than at mass 43 (due to CO_2 background in the detector), we counted long enough to insure that any mass 44 signal was at least ten times lower than the mass 43 signal. One possible explanation for the absence of acetaldehyde parent ion is that the acetaldehyde product might be highly vibrationally excited, resulting in a fragmentation pattern quite different from the known pattern at room temperature. Since the reaction $\text{CH}_3\text{CHO}^+ \rightarrow \text{CH}_2\text{CHO}^+ + \text{H}$ is only endothermic by 16 ± 2 kcal/mole,¹⁴ it is expected that acetaldehyde molecules containing a significant amount of internal energy will be incapable of forming stable parent molecular ions. We tried to

investigate this a little bit more by producing a molecular beam of acetaldehyde and measuring the mass 44 to 43 ratio in the direct beam at different nozzle temperatures. We measured a 44:43 ratio of 1.4 at room temperature. This ratio remained essentially constant up to a nozzle temperature of 850°C, where extensive reaction started to take place; we could not observe, in this limited range, any dependence of the fragmentation pattern on the internal excitation. We will discuss this point further in Sec. IV. For now, we will assume that acetaldehyde is actually the source of the $m/e = 43$ signal.

B. Product Energy Distributions

The laboratory angular and velocity distributions measured at $m/e = 43$ and $m/e = 42$ are used to derive the CM product translational energy distributions ($P(E)$'s) for rxns. (1) and (2). Experimental measurements at other, lower masses are also used to check whether the derived $P(E)$'s are correct and whether the assumption that we are dealing with the two dissociation channels (1) and (2) is plausible.

In attempting to fit our data, we start with a suitably parameterized total translational energy distribution which determines directly the CM velocity flux distribution for one product. Taking into account the velocity and two-dimensional angular distribution of the molecular beam we calculate the laboratory velocity flux distribution for the product at one certain angle. Then this distribution is convoluted over the finite length of the ionizer and finally compared to the measured TOF distribution, which has been nominally transformed to laboratory velocity space before. By varying the

parameters of the energy distribution and repeating these steps, a best fit translational energy distribution is derived. Theoretical total signals, as needed to calculate the angular distribution, are obtained by simply integrating the velocity distribution at several angles, taking into account the $1/v$ velocity dependence of the ionization probability.

In order to avoid complications due to several contributing products, we started the analysis with the acetaldehyde TOF distributions measured at $m/e = 43$. Figure 3 shows these distributions transformed to laboratory velocity space at three different angles. They were measured at a laser energy fluence of 1.8 J/cm^2 . We also measured mass 43 TOF distributions at different laser intensities. No dependence of the shape of the distributions on the laser intensity was observed for this product, suggesting that just one channel is contributing to the signal. The velocity distributions represented by the solid curves in Fig. 3 were calculated from a total translational energy distribution of the form

$$P(E) \propto (E-a)^n \exp(-E/b) \quad (3)$$

using the parameter values

$$\begin{aligned} n &= 3 \\ a &= -1 \\ b &= 8. \end{aligned} \quad (4)$$

The product translational energy distribution for rxn. (2) was derived from the velocity distributions for $m/e = 42$ shown in Fig. 4. At this mass we mainly observe the production of CH_2CHO radicals, but, as can be seen from the high velocity tail, we also have a little contribution from acetaldehyde. To minimize complications due to this interfering channel, we have chosen for evaluation the data where this contribution is minimal, namely, the data measured at our highest laser energy fluence (see Part C). Thus, in contrast to the measurements shown in Fig. 3, the data in Fig. 4 was taken at a fluence of 12 J/cm^2 .

The calculation allows for two contributing products, CH_2CHO and acetaldehyde. The latter is described by the translational energy distribution already derived (Eqns. (3) and (4)). For the production of $\text{CH}_2\text{CHO} + \text{C}_2\text{H}_5$, the total translational energy distribution was determined following the same procedure. Using the same form (3), we obtained as best fit parameters

$$\begin{aligned} n &= 2 \\ a &= -2 \\ b &= 2.33. \end{aligned} \tag{5}$$

The results of the calculation are displayed in Fig. 4 as solid curves whereas the dashed curves represent the individual contributions of CH_2CHO (left curve) and acetaldehyde (right curve with smaller amplitude). Observe that, with increasing angle, the acetaldehyde contribution gets more and more pronounced. The reason for this is only of a kinematic nature. Since

CH_2CHO is formed with much less translational energy than acetaldehyde, the laboratory angular distribution of CH_2CHO falls off much more quickly than that of acetaldehyde causing acetaldehyde to gain influence as the angle is increased. Such kinematic effects will also be encountered in other velocity distributions to be presented later.

Figure 5 shows the derived total translational energy distributions. The left solid curve represents the $P(E)$ for the dissociation products $\text{CH}_2\text{CHO} + \text{C}_2\text{H}_5$. They are formed with a mean translational energy of 5.3 kcal/mole. The dashed curve represents the $P(E)$ for the products of rxn. (1), acetaldehyde and ethylene. For this channel we find a mean translational energy of 31 kcal/mole, indicating that a large fraction of the exit barrier is converted into translational energy as the products recoil from the hexagonal transition state.

Figure 6 shows the velocity distributions measured at $m/e = 29$ together with the corresponding fits. The pronounced shoulder on the fast side at 5° and 20° is due to acetaldehyde which fragments in the ionizer to give CHO^+ . This contribution is dominant at 35° . The other two peaks are due to CH_2CHO (which also forms CHO^+) and its slightly faster counterpart C_2H_5 . The minor contribution of C_2H_5 is not obvious from the features shown in the velocity distributions, but its inclusion improves the fit. It should be emphasized that the peak areas for CH_2CHO and C_2H_5 relative to acetaldehyde are chosen free only at one angle; at the other angles this ratio is automatically determined by the calculated angular distributions.

At $m/e = 29$ we naturally cannot observe ethylene, the light counterpart of acetaldehyde, since its mass is $m = 28$. But ethylene is encountered in the velocity distributions measured at $m/e = 26$ (Fig. 7) where it gives rise to the fast peak at 3500–4000 m/s. The other contributions to $m/e = 26$ in Fig. 7 are C_2H_5 and a little CH_2CHO . Figures 6 and 7 demonstrate that the calculations based on the translational energy distributions derived for the heavy products fit the low mass data very well, too.

A final check is provided by the angular distributions. Figure 8 shows the measured and calculated laboratory angular distributions for acetaldehyde. Since the dissociation product is very fast (much faster than the average velocity of the molecular beam), and since the center-of-mass angular distribution is isotropic, we observe a laboratory angular distribution which is almost flat. We should mention that, for the analysis of the angular distributions measured with the less focussed laser beam (1.8 J/cm^2), we have accounted for the enlarged molecular beam–laser interaction region. The larger interaction region causes the angular distribution to fall off slightly faster since, at wide angles, the detector sees less of the interaction zone than at small angles. The inclusion of this detail in the calculation is the reason why the $m = 44$ curve in Fig. 8 is slightly different from that in Fig. 9.

The measured angular distribution for $m/e = 42$ is displayed in Fig. 9 by the open circles. As we know from the velocity distributions, we have to account for contributions from CH_2CHO and acetaldehyde in the calculation. The individual contributions of CH_2CHO ($m = 43$) and acetaldehyde ($m = 44$) to the $m/e = 42$ angular distribution are represented by the dashed curves in

Fig. 9. The relative contributions used to fit the $m/e = 42$ velocity distributions in Fig. 4 automatically fix the position of the $m = 44$ curve relative to the $m = 43$ curve. The sum of the separate contributions is represented by the upper solid curve and it is seen that this curve agrees very well with the measured points. The open triangles in Fig. 9 were obtained by integrating $m/e = 43$ TOF distributions measured at 12 J/cm^2 . These points provide an additional check of the calculated $m = 44$ angular distribution.

Another example is shown in Fig. 10. It displays measured and calculated angular distributions for $m/e = 29$. We have three contributions: acetaldehyde ($m = 44$), CH_2CHO ($m = 43$) and C_2H_5 ($m = 29$). The positions of the different curves relative to the $m = 43$ curve are determined by the fits to the $m/e = 29$ velocity distributions. The triangles were obtained by integrating $m/e = 43$ TOF distributions measured at 1.8 J/cm^2 . Although the agreement between measurement and calculation is not as good as for $m/e = 42$, it is still satisfactory. A similar result is obtained for $m/e = 26$, but because of its resemblance to Fig. 10 it will not be shown here.

Summarizing, we can state that the total translational energy distributions derived from the TOF measurements at $m/e = 43$ and $m/e = 42$ provide very good fits to the velocity distributions of the lower masses and to all measured angular distributions. This gives us confidence in our evaluation procedure and confirms the correctness of the derived energy distributions.

C. Branching Ratio

We also investigated, in a limited range, the dependence of the product branching ratio on the laser intensity. This was done by varying the position of the lens which focusses the laser beam onto the molecular beam. We measured, at three different lens positions, the ratio of the relative yields of acetaldehyde and CH_2CHO radicals detected at $m/e = 43$ and $m/e = 42$, respectively. These measurements were performed at a fixed detector angle of 10° . The results are given in Table 1 as $I(m = 42)/I(m = 43)$ vs. the energy fluence which, in our case, is proportional to the laser intensity since the temporal profile of the laser pulse has been kept constant. These values should not be taken absolutely, since the relative detection probabilities for the products have not been taken into account. Also, for the present purposes, the small contribution of acetaldehyde to the $m/e = 42$ signal has been ignored. The results indicate that as the laser intensity is increased the higher energy channel, producing free radicals, is favored more and more over the low energy channel. The effect is quite dramatic; the branching ratio changes by nearly a factor of five as the laser intensity is varied over one order of magnitude.

It is possible, in principle, to calculate absolute values of the product branching ratio from the ion signal ratios measured in the lab. The procedure, which has been described in detail in Ref. 11, involves calculating the true laboratory product ratio at a given angle from the measured ion signal ratios (taking into account differences in the ionization cross sections of the products, the product fragmentation patterns in the ionizer, and the variation of the quadrupole transmission with ion mass) and

then transforming this product ratio from the LAB to the CM coordinate system (using the product translational energy distributions for the competing channels). The major difficulty in the above procedure is usually determining the fragmentation patterns of the dissociation products in the ionizer. In a couple of cases this difficulty has been overcome, and absolute values have been obtained for the ratio of Cl vs. Cl₂ elimination from CF₂Cl₂,¹¹ and for the ratio of C-Cl vs. C-C bond fission in C₂F₅Cl.¹⁵

Unfortunately, the mass spectroscopy is a lot messier in the case of EVE, due to the large number of hydrogens. The signal observed at almost every ion mass involves contributions from two or more dissociation products. We did not attempt to unravel these individual contributions at all important ion masses. Hence the ionizer fragmentation patterns of the products are not well known and the branching ratio cannot be determined accurately.

Still, we would like to report one calculation which serves to illustrate the purely kinematic effect of the LAB → CM transformation on the product ratio. We will (arbitrarily) assume that the fraction of acetaldehyde molecules entering the detector which form m/e = 43 ions is equal to the fraction of CH₂CHO radicals which form m/e = 42 ions. Then the I(m = 42)/I(m = 43) ratios in Table 1 are equal to the true laboratory CH₂CHO: CH₃CHO ratios at 10°. Transforming to the CM as described in Appendix II of Ref. 11, we find that the fraction of the total dissociation yield which proceeds through the higher energy channel (2) is 14, 31 and 43 at energy fluences of 0.7, 1.8 and 12 J/cm², respectively.

IV. DISCUSSION

The discovery of the phenomenon of infrared multiphoton absorption has generated renewed interest in the study of unimolecular reactions. The three general classes of unimolecular reactions are: (1) simple fission reactions, in which a single chemical bond is broken and no new bonds are formed in the products; (2) complex fission reactions, in which bonds are broken and formed simultaneously; (3) isomerization reactions. The first class has been most extensively studied. Molecular beam experiments¹⁶ on a variety of simple fission reactions have shown that, in all cases, the products are formed with a statistical translational energy distribution. While this evidence helps support the hypothesis that energy is randomized in the molecules prior to dissociation, the dynamics are too trivial to be very interesting.

More interesting from a dynamical standpoint are the complex fission and isomerization reactions. Unlike the simple fission reactions, these reactions generally involve substantial potential energy barriers in the exit channel (these barriers show up as activation energies for the reverse association or isomerization reactions). The isomerization reactions are not easily studied by molecular beam methods. We will restrict our attention here to the complex fission reactions.

RRKM theory assumes a statistical partitioning of energy between the reaction coordinate and internal degrees of freedom in the critical configuration. In most simple fission reactions there is very little interaction between the products after the critical configuration is passed, and so the product energy distribution will reflect the statistical distribution at the critical configuration. However, the products of a

complex fission reaction are expected to interact strongly as they descend the exit channel barrier, and the asymptotic product energy distribution may look very different from the energy distribution seen at the top of the barrier. Insight into these exit channel effects may be obtained by determining how the barrier energy is partitioned between the various product degrees of freedom. Some progress has been made in this direction.

Using the crossed laser-molecular beam method, Sudbo et al.¹⁷ obtained product translational energy distributions for a number of reactions involving three- and four-center HCl elimination from halogenated hydrocarbons. They found that, in the four-center reactions, only a small fraction of the exit barrier energy is converted to product translation. (For example, in the reaction $\text{CH}_3\text{CCl}_3 \rightarrow \text{CH}_2\text{CCl}_2 + \text{HCl}$, less than 20 of the 42 kcal/mole barrier is released as product translation.) However, in the three-center elimination of HCl from CF_2HCl , more than half of the 6-7 kcal/mole barrier enters product translation. A similar efficient conversion of exit barrier potential energy into product translational energy has been observed in the three-center elimination of Cl_2 from CF_2Cl_2 .¹¹ While molecular beam experiments so far have mainly yielded information on product translational energy distributions, other techniques have been applied in gas cells to deduce the internal energy distributions of products from complex fission reactions. Examples include the determination of relative HF vibrational populations in four-center HF elimination reactions by monitoring infrared fluorescence,¹⁸ and the use of UV laser-induced fluorescence to probe the rotational and vibrational energy distributions of CF_2 radicals

produced in the three-center elimination reactions of CF_2HCl , CF_2Cl_2 and CF_2Br_2 .¹⁹

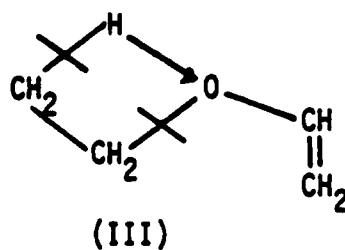
The intramolecular rearrangement reaction of EVE is a somewhat more exotic example of a complex fission reaction. Three electron pair bonds are broken and three bonds are formed in a single, concerted process. The height of the exit barrier for this reaction is 38 kcal/mole. The acetaldehyde and ethylene products are formed with a mean translational energy of 31 kcal/mole. RRKM calculations (to be described later) suggest that the EVE molecules dissociate from levels of excitation 40–70 kcal/mole above the threshold for rxn. (1). Of this excess energy, only 6%, or 2–4 kcal/mole, is predicted to enter product translation. Therefore it appears that a very large fraction (roughly 70%) of the exit channel barrier is converted into product translational energy.²⁰ In view of the fact that both dissociation products are fairly large polyatomic molecules with many vibrational degrees of freedom, it is rather surprising that such a large fraction of the barrier energy can be funneled into the translational coordinate. Evidently, when the H atom transfers and the C–O bond breaks, an enormous repulsive force is created which rapidly drives the acetaldehyde and ethylene products apart without exciting product vibrational motion.

The subject of energy disposal may also be relevant to the question of why we did not observe acetaldehyde parent ions in this experiment. We know that the fixed energy of the barrier mainly appears as product translational energy. Even so, the products are expected to contain quite a bit of vibrational energy, since most of the estimated 40–70 kcal/mole of excess energy remains in the internal degrees of freedom of the products. The

acetaldehyde product probably contains, on average, at least 30 kcal/mole of vibrational energy, which would seem to be sufficient to preclude the formation of stable acetaldehyde parent ions (unless significant amounts of vibrational energy are removed in the electron bombardment ionization process, which is unlikely for such a large molecule).

We are still somewhat disturbed that, when we used the mass spectrometer to monitor a molecular beam of acetaldehyde, we could not detect any significant change in the mass 44:43 ion ratio as the nozzle temperature was varied between room temperature and 850°C (see Sec. IIIA). At 850°C, the average vibrational energy content of an acetaldehyde molecule is ~12 kcal/mole. (While some vibrational relaxation is expected to occur during the supersonic expansion, this is probably not too important.) If the reaction $\text{CH}_3\text{CHO}^+ \rightarrow \text{CH}_3\text{CO}^+ + \text{H}$ is really only endothermic by 16 ± 2 kcal/mole,¹⁴ we ought to see some decrease in the mass 44:43 ratio as the acetaldehyde is heated. Perhaps such a decrease is actually occurring, but is coincidentally balanced by additional sources of mass 44 ions which are produced in the nozzle by radical chain reactions.

One other possible explanation of our failure to observe acetaldehyde parent ions in the multiphoton dissociation of EVE might be mentioned. Suppose that the intramolecular rearrangement proceeds through the following intermediate:



This reaction would produce ethylene and the vinyl alcohol tautomer of acetaldehyde. In the pyrolysis experiments, the vinyl alcohol would be rapidly converted, through collisions, to acetaldehyde (which is more stable by ~ 10 kcal/mole²¹). However, in the collisionless molecular beam environment, the vinyl alcohol primary product might be incapable of overcoming the barrier to isomerization, and survive to reach the detector. "Enol" tautomers typically produce much less parent ion on electron impact than their "keto" counterparts. Therefore, if vinyl alcohol is produced, the absence of $m/e = 44$ signal would not be so surprising.

Unfortunately, this interpretation of the rearrangement reaction in terms of intermediate (III) has some problems of its own. If vinyl alcohol is formed instead of acetaldehyde, the exit barrier is reduced from 38 kcal/mole to ~ 28 kcal/mole. This makes it harder to explain the large amount of translational energy observed in the products. Also, the extremely low A-factor observed in the pyrolysis experiments is probably more consistent with the hexagonal intermediate (II), in which all internal rotations are lost, than with intermediate (III), which retains one internal rotational degree of freedom. Nevertheless, we do not believe that intermediate (III) can be completely ruled out on the basis of the existing experimental evidence. Radioactive labeling experiments would not be able to distinguish between intermediates (II) and (III). Still, it might be possible to determine whether acetaldehyde or vinyl alcohol is the true primary product by using some real-time spectroscopic technique in a shock-tube or molecular beam experiment.

We would like to turn our attention now to the competing reaction channel (2). Although the average recoil energy is low in this case, the distribution of recoil energies peaks at a finite value. At first this might seem odd, since rxn. (2) looks like a simple bond fission reaction. However, since the C-O bond in the CH_2CHO fragment acquires considerable double-bond character⁶ as the $\text{C}_2\text{H}_5\text{-O}$ bond breaks, rxn. (2) should more properly be viewed as a complex fission reaction and may involve a small exit barrier. (The situation is analogous to H-elimination from $\text{C}_2\text{H}_4\text{F}$ radicals,²² where a C-C double bond forms as H departs. This reaction involves an exit barrier of ~ 4 kcal/mole, most of which is converted to product translational energy.) We suspect, therefore, that there exists a small but finite activation energy for the recombination of CH_2CHO and C_2H_5 radicals.

The fact that rxn. (2) is observed at all, even though its energy threshold lies ~ 20 kcal/mole above that for rxn. (1), is due to the greatly different A-factors for the two reactions. In the language of Transition State Theory, rxn. (1) has a much larger (negative) entropy of activation than rxn. (2), which partially offsets the difference in activation energies in determining the relative rate constants for these competing channels. We investigated this competition somewhat more quantitatively in the context of RRKM theory. It is known that the shape of an RRKM rate constant vs. energy curve is insensitive to the exact choices of the molecular and critical configuration frequencies as long as these frequencies are chosen to reproduce the thermal A-factor for the reaction.²³ The A-factor for rxn. (1) is $\log_{10} A_1 = 11.6$. Although the A-factor for rxn. (2) has not been experimentally determined, Rosenfeld et al.⁷ have estimated that

$\log_{10} A_2 = 15$ using Benson's group additivity rules.⁵ This is a reasonable value. Choosing frequencies which reproduced these A-factors, and assuming threshold energies of 44 kcal/mole and 66 kcal/mole for rxns. (1) and (2), respectively, we calculated the RRKM rate constant curves shown in Fig. 11.

How will the average excitation energy (and hence the branching ratio) depend on the laser intensity and energy fluence? According to the rate equation model for multiphoton absorption and dissociation, two limiting cases should be considered.²⁴ If the laser energy fluence is low, such that very few molecules dissociate until after the laser pulse is over, then the average level of excitation from which the molecules dissociate will increase with increasing energy fluence, but will be independent of laser intensity for a given fluence. However, at sufficiently high values of the energy fluence, the molecules will continue to absorb photons until the dissociation rate becomes competitive with the excitation rate. Then, most of the dissociation will occur during the laser pulse, and the average level of excitation of dissociating molecules will depend mainly on the laser intensity. For typical 100 ns TEA laser pulses, maximum excitation rates (and hence maximum dissociate rates) on the order of $10^8 - 10^9 \text{ s}^{-1}$ are expected. In the fluence range of the present experiments, we are probably in the transition region between fluence-limited and intensity-limited excitation.

Due to the finite residence time of excited molecules in the region viewed by the detector, we are mainly sensitive to molecules with dissociation lifetimes shorter than a few microseconds. The RRKM rate constant for

rxn. (1) reaches 10^6 s^{-1} for excitation energies around 80 kcal/mole (35 kcal/mole above the threshold for rxn. (1)). At this level of excitation the higher energy channel is predicted to account for 4% of the total dissociation yield. As is obvious from Fig. 11, the RRKM branching ratio shifts dramatically in favor of the radical producing channel as the excitation energy is increased. At ~100 kcal/mole the rates of rxns. (1) and (2) are equal, and at very high excitation energies rxn. (2) will completely dominate over rxn. (1). Although we were unable to extract absolute values of the branching ratio in the present experiment, the results in Table 1 clearly indicate the shift of the branching ratio in favor of rxn. (2) as the laser intensity and energy fluence are increased, in agreement with the considerations outlined above.

As mentioned in the introduction, Brenner⁸ also studied the dependence of the EVE product branching ratio on laser intensity. He compared product yields in a gas cell using laser pulses of constant energy fluence but different durations. At both 0.56 and 0.91 J/cm², he observed only the products of rxn. (1) with the "long" (2 μs) laser pulses, while comparable yields from rxns. (1) and (2) were found with the "short" (0.2 μs) pulses. (In Brenner's experiment, the pulse duration was varied by changing the N₂ content in the laser. Removing the N₂ from the gas mix eliminates the ~2 μs long tail from the TEA laser pulse, without altering the shape of the initial 200 ns long spike. (See Fig. 1 of Brenner's paper.) Therefore the difference in peak intensity between Brenner's "short" and "long" pulses, for the same total pulse energy, is probably not more than a factor of two or three.) However, Brenner also reported that the relative yields of rxns. (1)

and (2) (with the 0.2 μ s pulses) were the same, within experimental error, at 0.56 and 0.91 J/cm². On the one hand, Brenner's results suggest that the branching ratio changes by more than two orders of magnitude as the laser intensity is changed by a factor of two (at constant fluence), while when the fluence and intensity are increased together by about a factor of two, the branching ratio remains nearly constant. Our results clearly show that, as the energy fluence and intensity are increased together, the branching ratio shifts in favor of rxn. (2). Brenner's results do not appear to be internally consistent. They cannot reflect the primary photochemistry. We certainly do not understand how Brenner can conclude from his results that "during laser pumping a statistical energy distribution may not be realized when $\tau_p = 0.2 \mu$ s." In fact, the branching ratio behavior we observe is, at least qualitatively, exactly what one would expect on the basis of the statistical theory of unimolecular reactions.

ACKNOWLEDGMENTS

This work was supported by the Office of Naval Research under contract number N00014-75-C-0671. F.H. acknowledges a Fellowship from the Max-Planck-Gesellschaft, Munchen, Federal Republic of Germany.

REFERENCES

- a. Permanent address: Max-Planck-Institut für Stromungsforschung, D-3400 Göttingen, Federal Republic of Germany.
- b. Also associated with the Department of Chemistry, University of California, Berkeley, California 94720.
- c. Permanent address: Physics Department, Fudan University, Shanghai, People's Republic of China.
- d. Also associated with the Department of Physics, University of California, Berkeley, California 94720.
- e. Miller Professor, 1981-1982.
1. S.-N. Wang and C.A. Winkler, Can. J. Res. 21, 97 (1943).
2. A.T. Blades and G.W. Murphy, J. Am. Chem. Soc. 74, 1039 (1952).
3. M.J. Molera, J.M. Gamboa, J.A. Garcia Dominquez and A. Couto, J. Gas Chromatography 6, 594 (1968).
4. S.W. Benson and H.E. O'Neal, Kinetic Data on Gas Phase Unimolecular Reactions, Natl. Stand. Ref. Data Ser., U.S. Natl. Bur. Stand. 21 (U.S. Government Printing Office, Washington, D.C., 1970).
5. S.W. Benson, Thermochemical Kinetics, 2nd ed. (Wiley, New York, 1976).
6. G. Inoue and H. Akimoto, J. Chem. Phys. 74, 425 (1981).
7. R.N. Rosenfeld, J.I. Brauman, J.R. Barker and D.M. Golden, J. Am. Chem. Soc. 99, 8063 (1977).
8. D.M. Brenner, Chem. Phys. Lett. 57, 357 (1978).
9. Y.T. Lee, J.D. McDonald, P.R. LeBreton and D.R. Herschbach, Rev. Sci. Instrum. 40, 1402 (1969).
10. N.L. Owen and N. Sheppard, Spectrochim. Acta 22, 1101 (1966).

11. D. Krajnovich, F. Huisken, Z. Zhang, Y.R. Shen and Y.T. Lee, J. Chem. Phys., in press.
12. R.J. Buss, R.J. Baseman, G.Z. He and Y.T. Lee, J. Photochem. 17, 389 (1981).
13. Atlas of Mass Spectral Data, Vol. 1, E. Stenhagen, S. Abrahamsson and F.W. McLafferty, eds. (Wiley, New York, 1969).
14. R. Kraßig, D. Reinke and H. Baumgartel, Ber. Bunsenges. Phys. Chem. 78, 425 (1974). These workers obtain, from appearance potential measurements, $\Delta H_{f298}^0(C_2H_4O^+) = 196.0 \pm 0.5$ kcal/mole and $\Delta H_{f298}^0(C_2H_3O^+) = 160 \pm 1$ kcal/mole.
15. Unpublished results from this laboratory.
16. Aa.S. Sudbo, P.A. Schulz, E.R. Grant, Y.R. Shen and Y.T. Lee, J. Chem. Phys. 70, 912 (1979).
17. Aa.S. Sudbo, P.A. Schulz, Y.R. Shen and Y.T. Lee, J. Chem. Phys. 69, 2312 (1978).
18. C.R. Quick, Jr. and C. Wittig, J. Chem. Phys. 72, 1694 (1980).
19. D.S. King and J.C. Stephenson, Chem. Phys. Lett. 51, 48 (1977); J.C. Stephenson and D.S. King, J. Chem. Phys. 69, 1485 (1978).
20. We have implicitly assumed that it is possible to treat the "fixed" energy of the barrier and the "non-fixed" energy in excess of the barrier on separate dynamical footings. That is, we have assumed that the "fixed" energy is partitioned among the product degrees of freedom in a unique way, and that the "non-fixed" energy, which according to RRKM theory is statistically distributed in the critical configuration, remains statistically distributed in the products. While this separate

treatment of the "fixed" and "non-fixed" energies is somewhat arbitrary and artificial, the fact that we observed no significant change in the product translational energy distribution for rxn. (1) as the laser intensity (and hence the average level of excitation) was varied supports the conclusion that the "fixed" energy of the barrier is largely responsible for the observed translational energy release.

21. S. Forsen and M. Nilsson, "Enolization", in The Chemistry of the Carbonyl Group, Vol. 2, J. Zabicky, ed. (Wiley, New York, 1970).
22. J.M. Parson and Y.T. Lee, J. Chem. Phys. 56, 4658 (1972).
23. P.J. Robinson and K.A. Holbrook, Unimolecular Reactions (Wiley, New York, 1972).
24. P. A. Schulz, Ph.D. Thesis, University of California, Berkeley, California (1979).

Table 1. Mass 42 to 43 ion signal ratio measured at a laboratory deflection angle of 10° vs. laser energy fluence.

Energy Fluence (J/cm ²)	$\frac{I(m = 42)}{I(m = 43)}$
0.7	1.6
1.8	4.4
12	7.2

FIGURE CAPTIONS

- Fig. 1. Energetics of some possible EVE decomposition channels calculated using thermochemical data. An approximate heat of formation of EVE was taken from Ref. 4. Product heats of formation (except $\text{CH}_2\text{CHOCH}_2$) were taken from Ref. 5. (The enthalpy change for the CH_3 elimination reaction was guessed.) The rearrangement reactions leading to $\text{CH}_2\text{CO} + \text{C}_2\text{H}_6$ and $\text{CH}_3\text{CHCH}_2 + \text{CH}_2\text{O}$ are expected to involve large exit channel barriers.
- Fig. 2. Time-of-flight distributions of $m/e = 43, 42$ and 26 measured at 20° from the molecular beam at a laser energy fluence of 1.8 J/cm^2 . The dots represent the actual data. The curves are not fits, and are merely intended to guide the eye. The distance from the interaction region to the center of the ionizer is 21.1 cm . The time scale has not been adjusted for the flight time of the ions through the mass spectrometer ($16 \text{ } \mu\text{s}$ for $m/e = 26$, $21 \text{ } \mu\text{s}$ for $m/e = 43$). The arrow marks the flight time corresponding to the EVE beam velocity.
- Fig. 3. Laboratory velocity flux distributions of acetaldehyde at 1.8 J/cm^2 . \bigcirc Experimental points ($m/e = 43$ monitored by the mass spectrometer). The curves were calculated from the dashed-line $P(E)$ in Fig. 5.
- Fig. 4. Velocity flux distribution of the $m/e = 42$ mass spectrometer signal at 12 J/cm^2 . \bigcirc Experimental points; — Best fit, obtained by adding the individual contributions (dashed curves) of CH_2CHO and acetaldehyde to the $m/e = 42$ signal. The individual contributions of CH_2CHO and acetaldehyde were calculated from the $P(E)$'s shown in Fig. 5.

Fig. 5. Derived center-of-mass product translational energy distributions for both dissociation channels. The distributions are of the

form $P(E) = (E-a)^n \exp(-E/b)$ with

----- $n = 3, a = -1, b = 8;$

_____ $n = 2, a = -2, b = 2.33.$

Fig. 6. Measured and calculated velocity flux distributions of the $m/e = 29$ mass spectrometer signal at 1.8 J/cm^2 . The calculation accounts for the production of acetaldehyde (fast curve) and CH_2CHO (slow curve) and a minor contribution from C_2H_5 .

Fig. 7. Measured and calculated velocity flux distributions of the $m/e = 26$ mass spectrometer signal at 1.8 J/cm^2 . The main contributions in the calculated curves are fast C_2H_4 and slow C_2H_5 , with a small contribution from CH_2CHO .

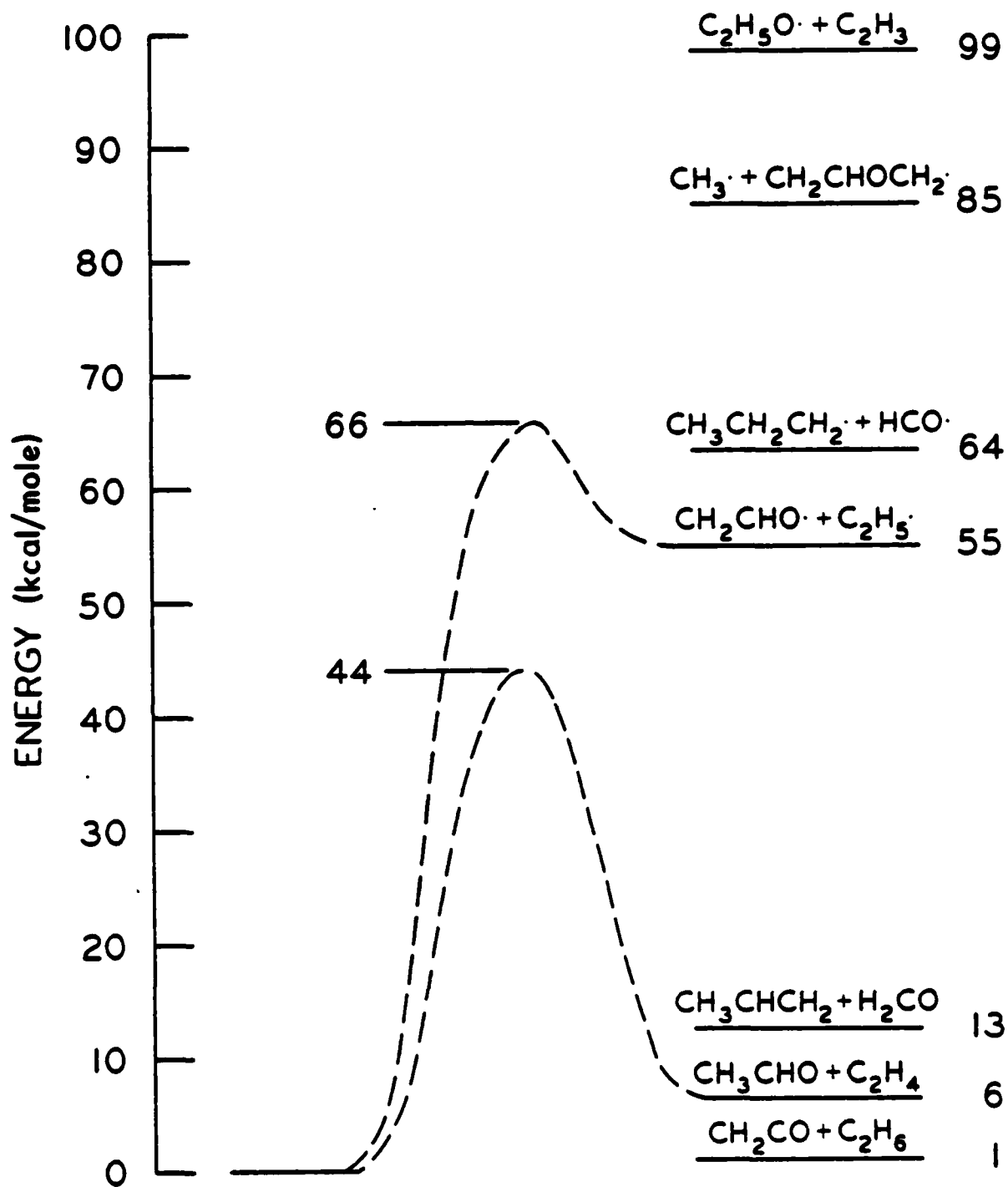
Fig. 8. Laboratory angular distribution of acetaldehyde at 1.8 J/cm^2 .

○ Experimental points (measured at $m/e = 43$). Error bars represent plus and minus one standard deviation of the statistical counting error. _____ Calculated from the dashed-line $P(E)$ in Fig. 5.

Fig. 9. Laboratory angular distribution of the $m/e = 42$ mass spectrometer signal at 12 J/cm^2 . ○ Experimental points; _____ distribution calculated using the same relative contributions of CH_2CHO ($m = 43$) and acetaldehyde ($m = 44$) that were used to fit the $m/e = 42$ velocity distributions. The triangles represent the contribution of acetaldehyde as obtained by integrating $m/e = 43$ TOF distributions measured at 12 J/cm^2 .

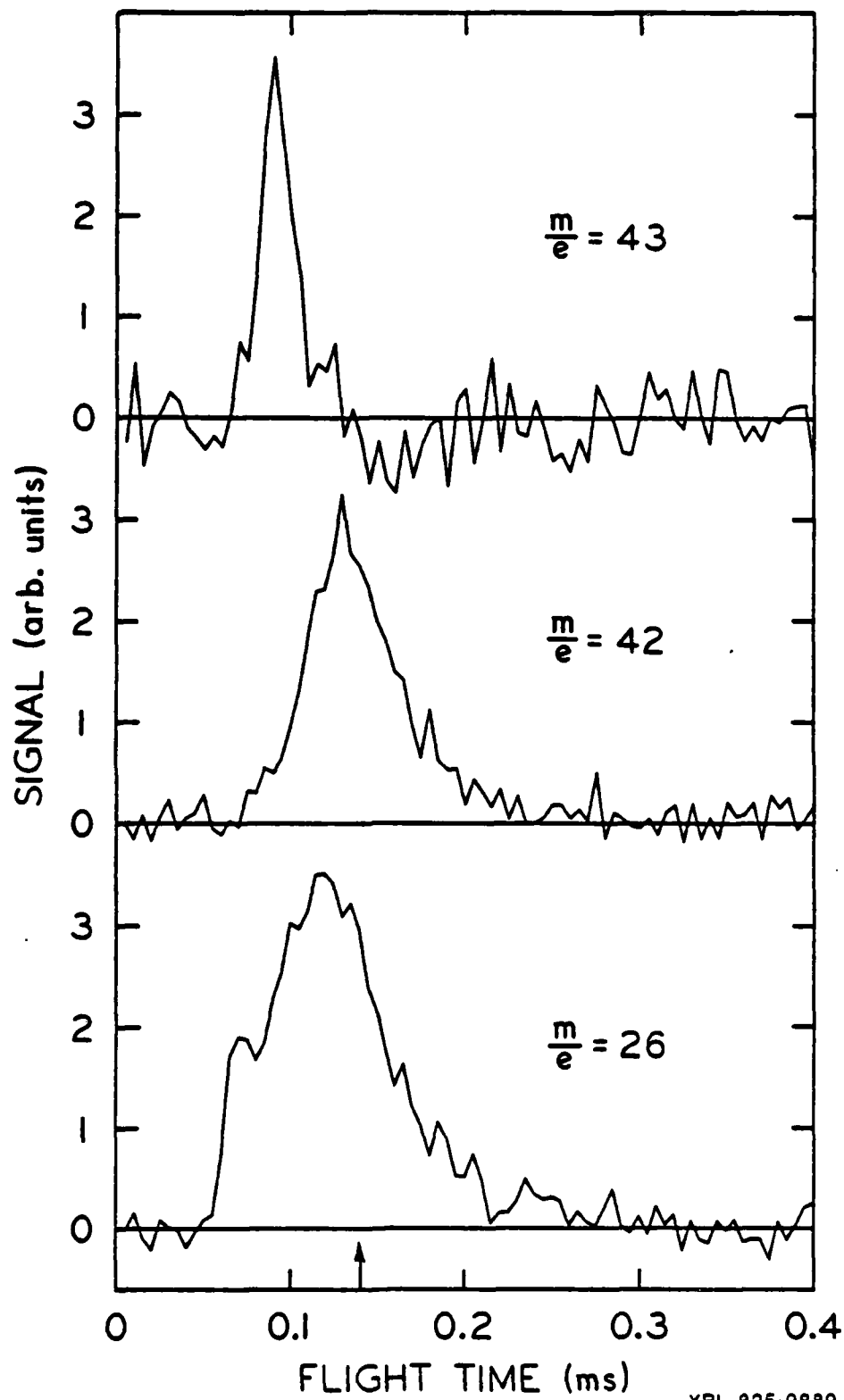
Fig. 10. Laboratory angular distribution of the $m/e = 29$ mass spectrometer signal at 1.8 J/cm^2 . \bigcirc Experimental points; — distribution calculated using the same relative contributions of CH_2CHO ($m = 43$), acetaldehyde ($m = 44$) and C_2H_5 ($m = 29$) which were used to fit the $m/e = 29$ velocity distributions. The triangles represent the contribution of acetaldehyde as obtained by integrating $m/e = 43$ TOF distributions measured at 1.8 J/cm^2 .

Fig. 11. RRKM rate constant curves for EVE decomposition, assuming $E_0 = 44 \text{ kcal/mole}$, $\log_{10} A = 11.6$ for the reaction producing $\text{CH}_3\text{CHO} + \text{C}_2\text{H}_4$, and $E_0 = 66 \text{ kcal/mole}$, $\log_{10} A = 15$ for the reaction producing $\text{CH}_2\text{CHO} + \text{C}_2\text{H}_5$.



XBL 825-9887

Fig. 1



XBL 825-9889

Fig. 2

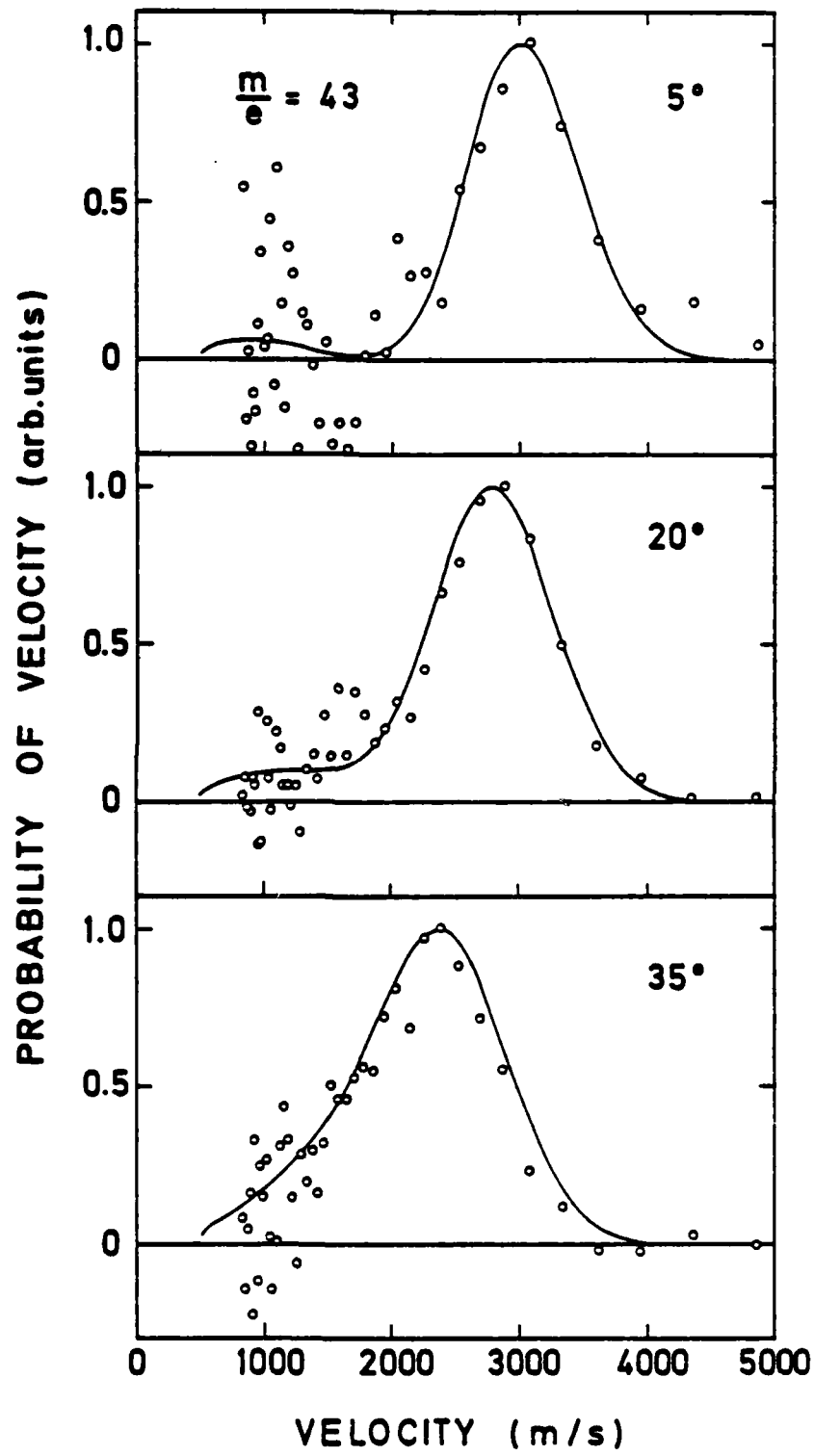


Fig. 3

XBL 8010-12500

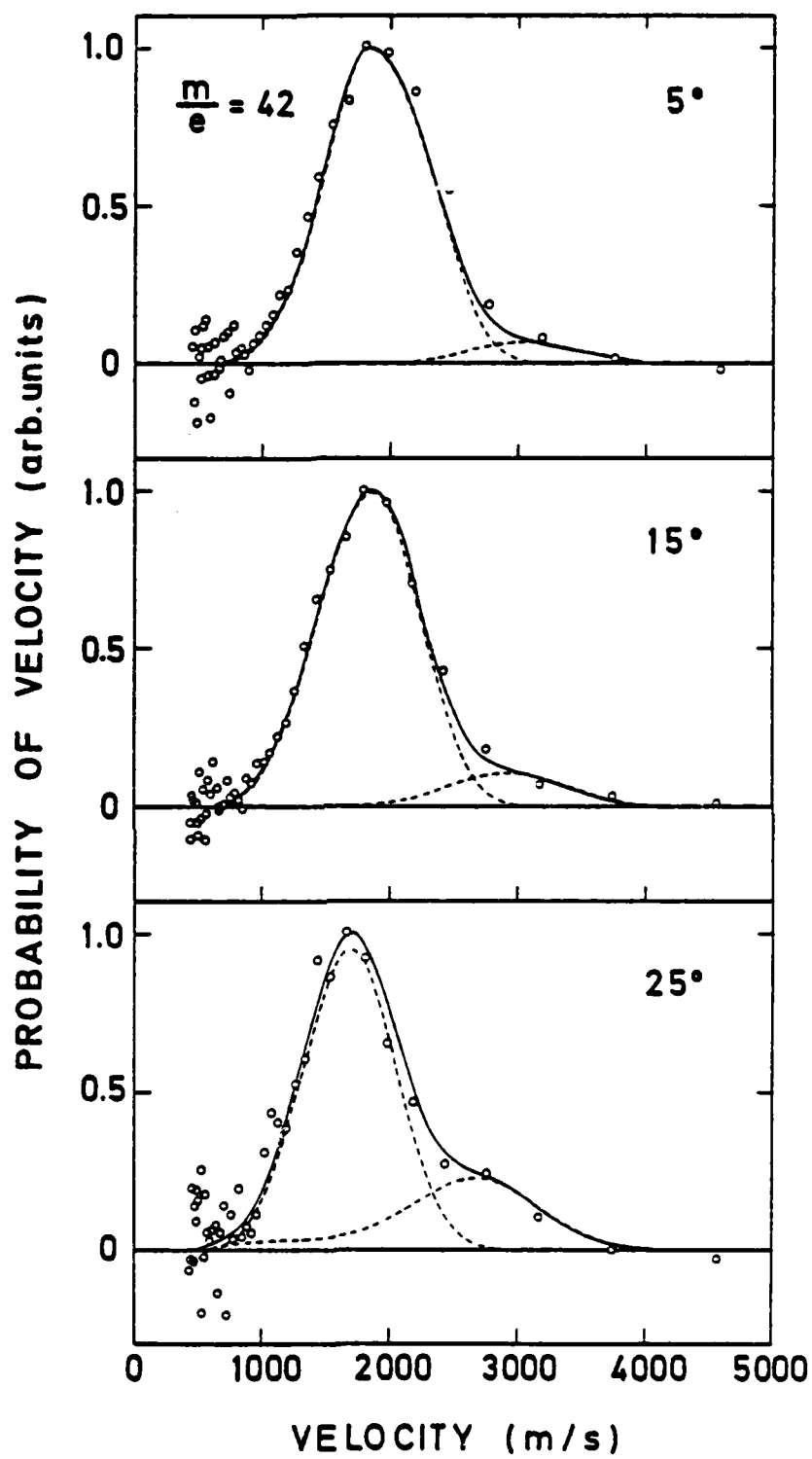
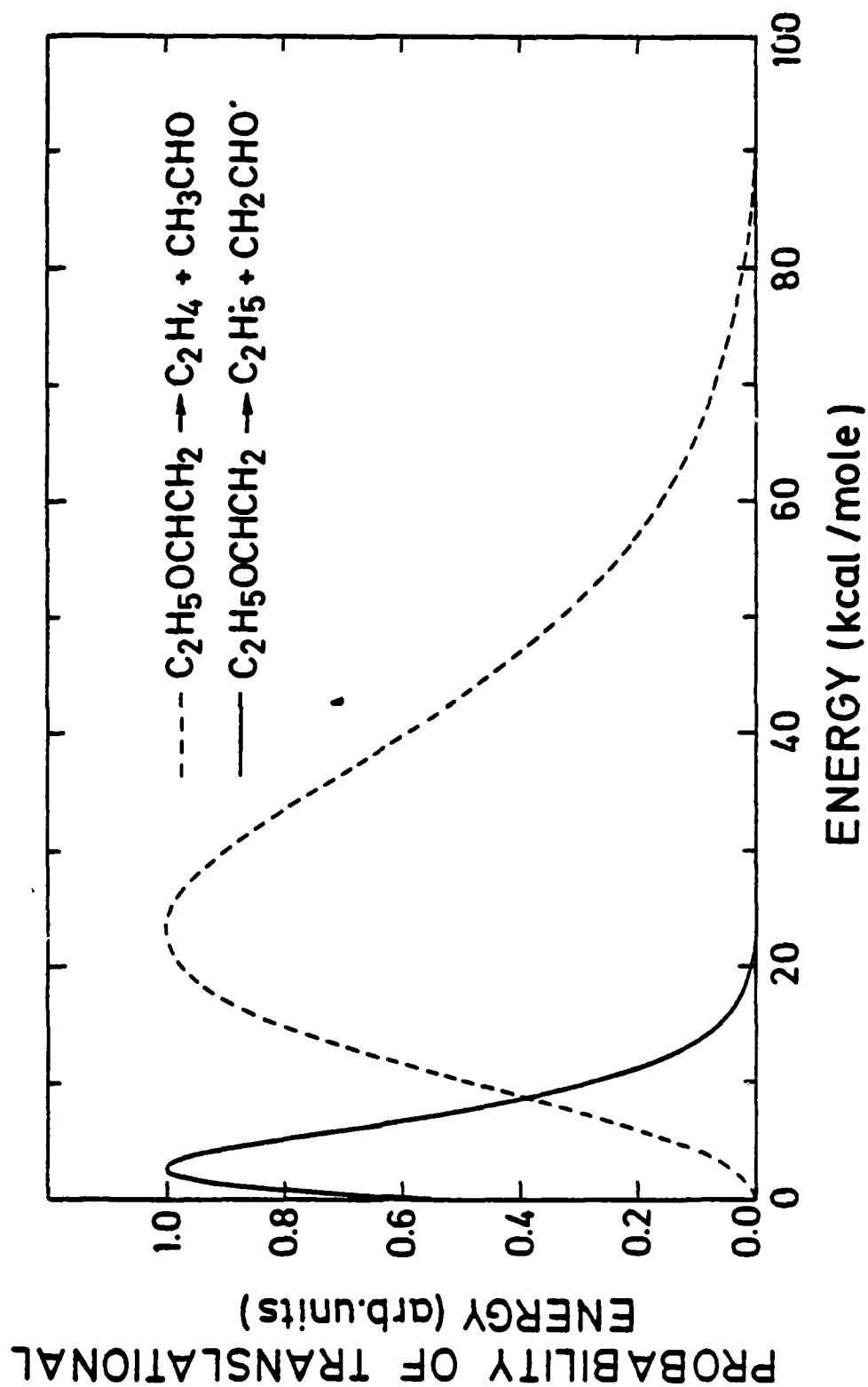


Fig. 4

XBL 8010-12501



XBL 8010-12496

Fig. 5

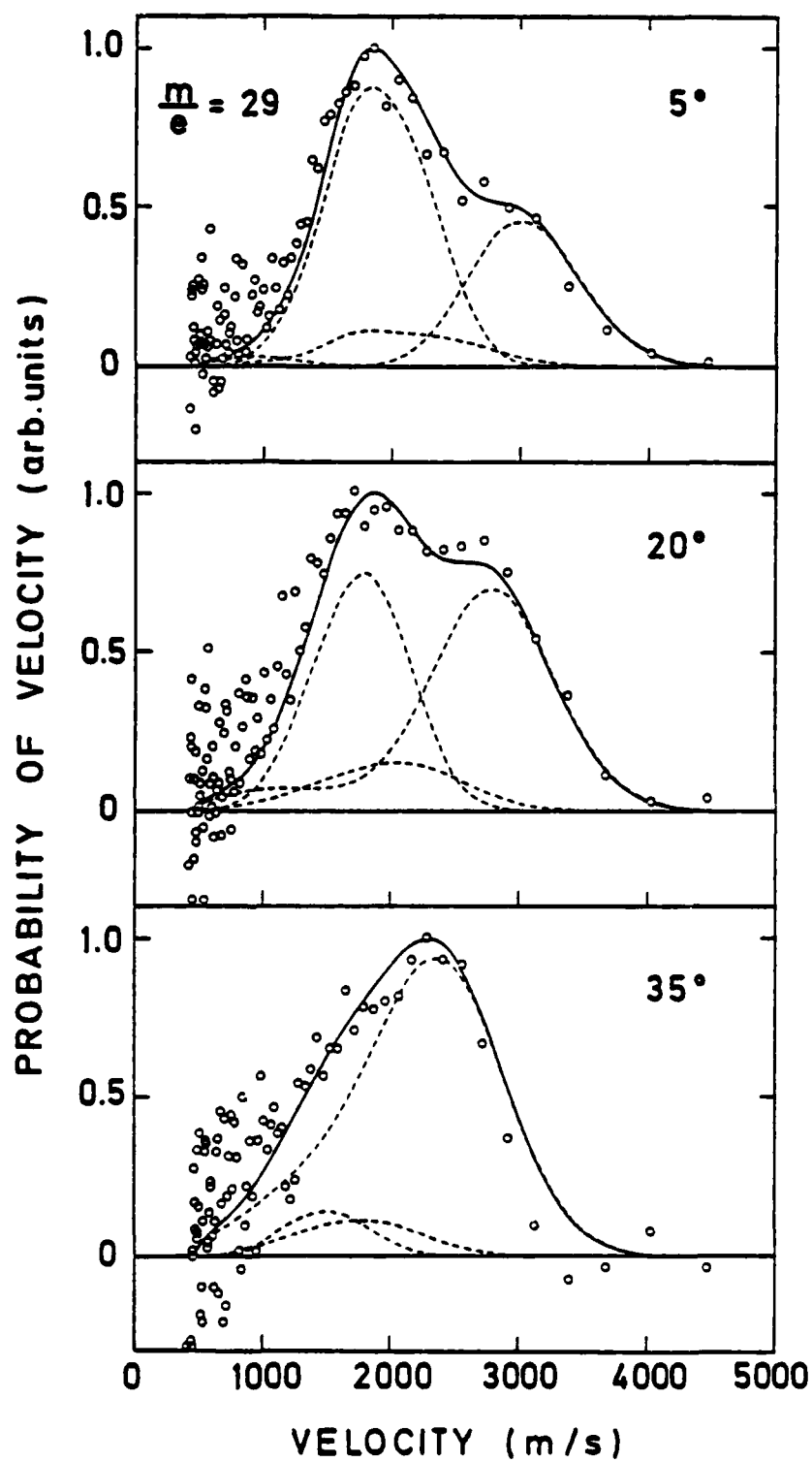


Fig. 6

XBL 8010-12502

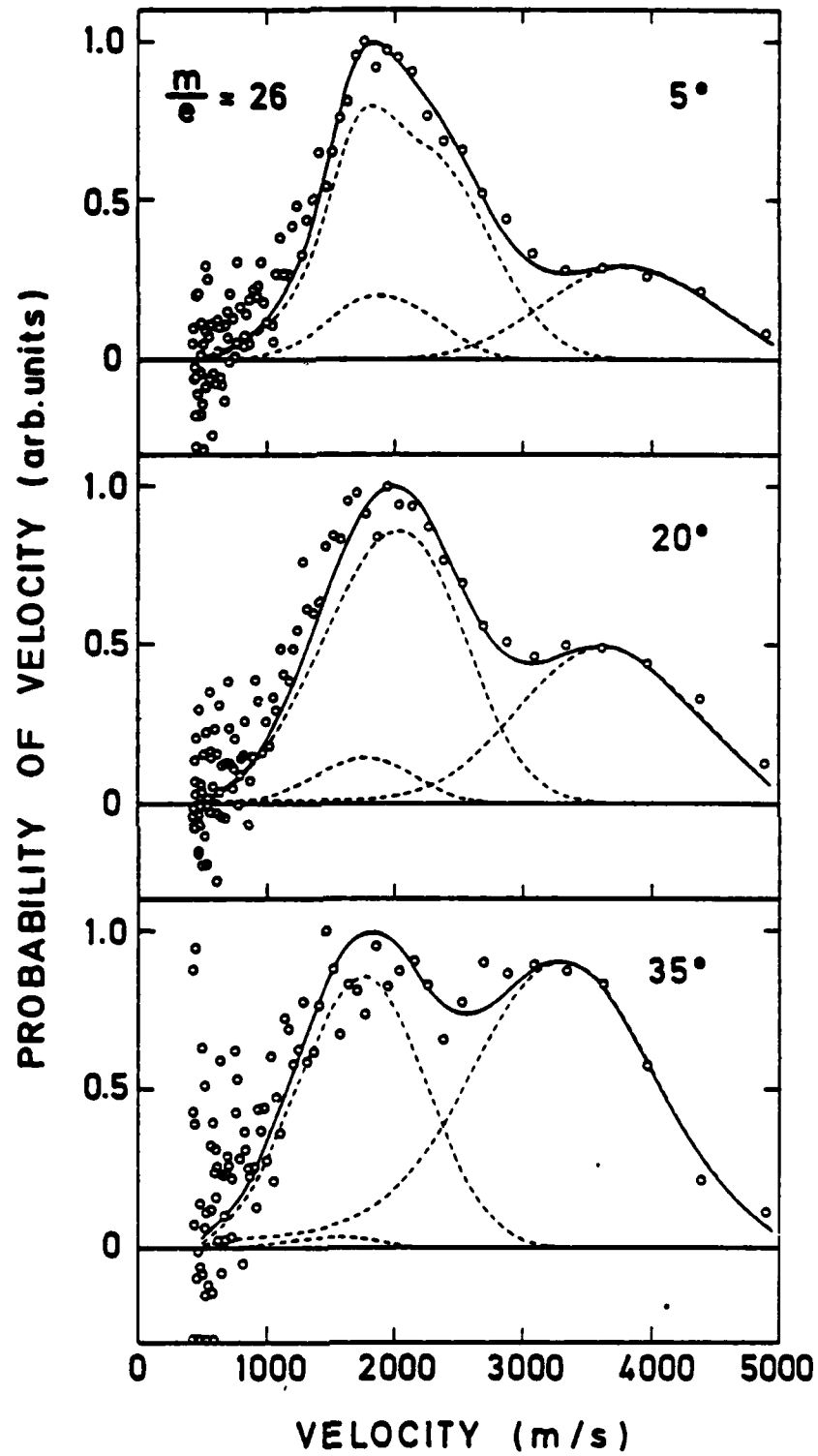


Fig. 7

XBL 8010-12503

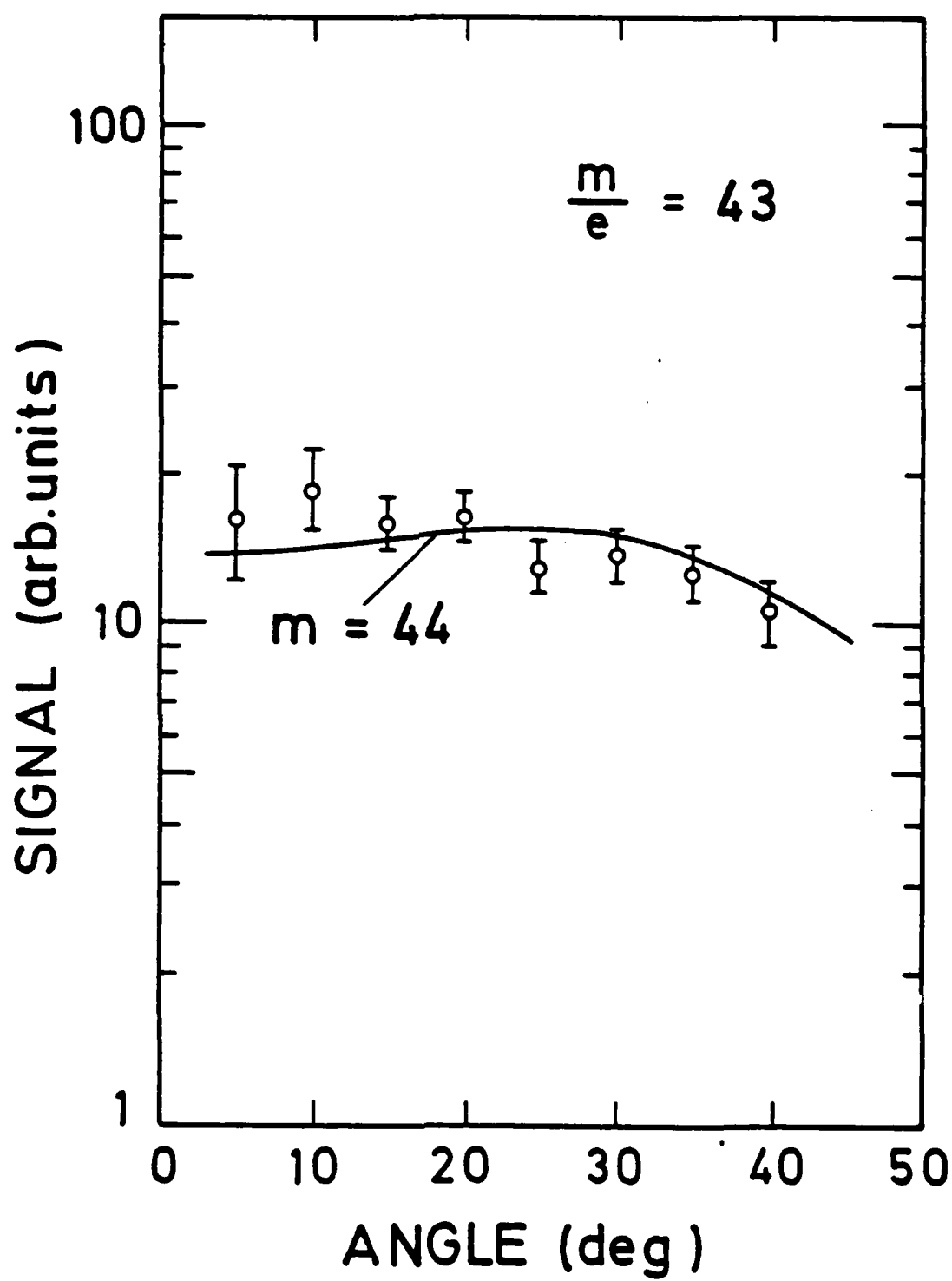


Fig. 8

XBL 8010-12497

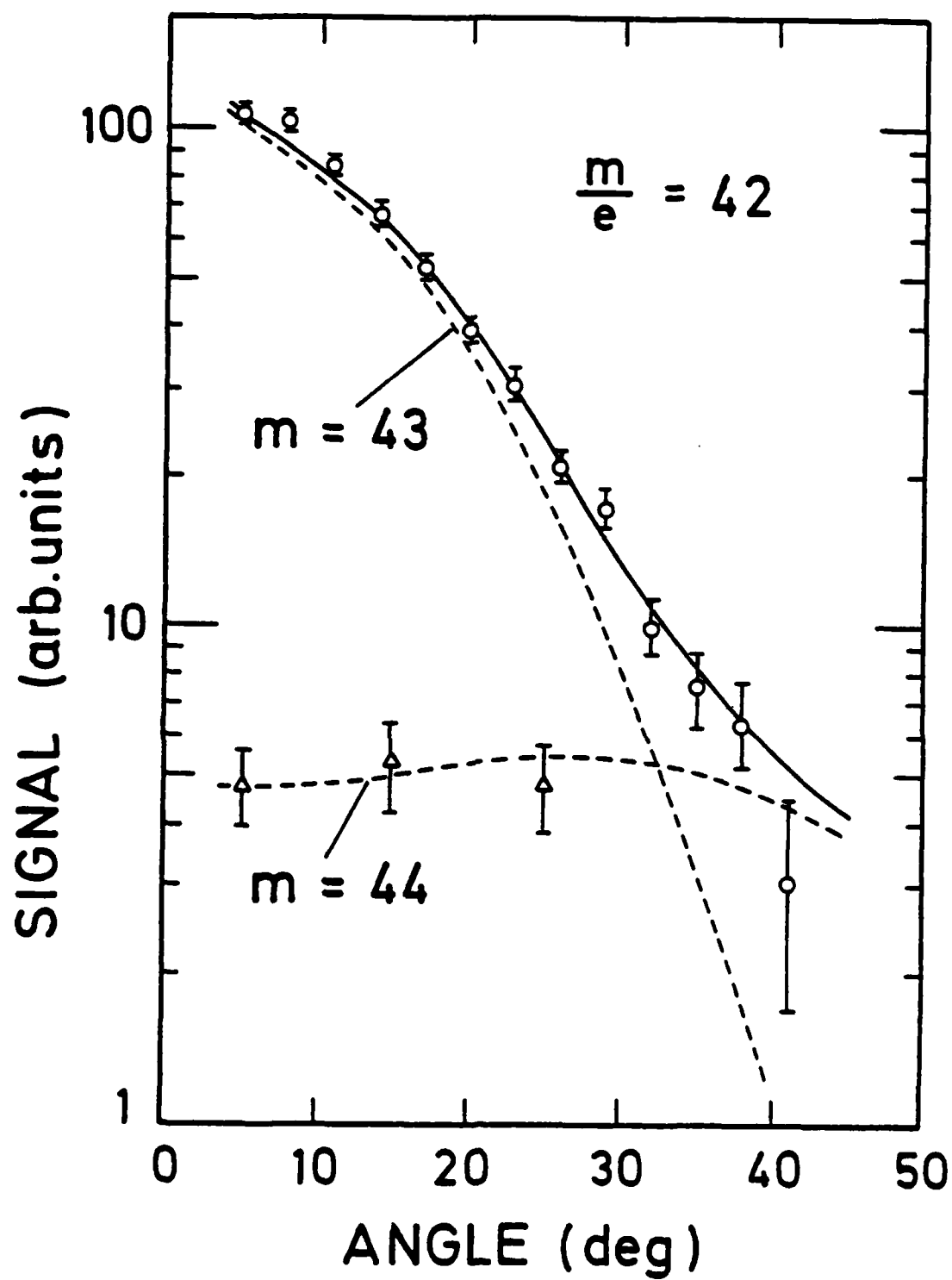


Fig. 9

XBL 8010-12498

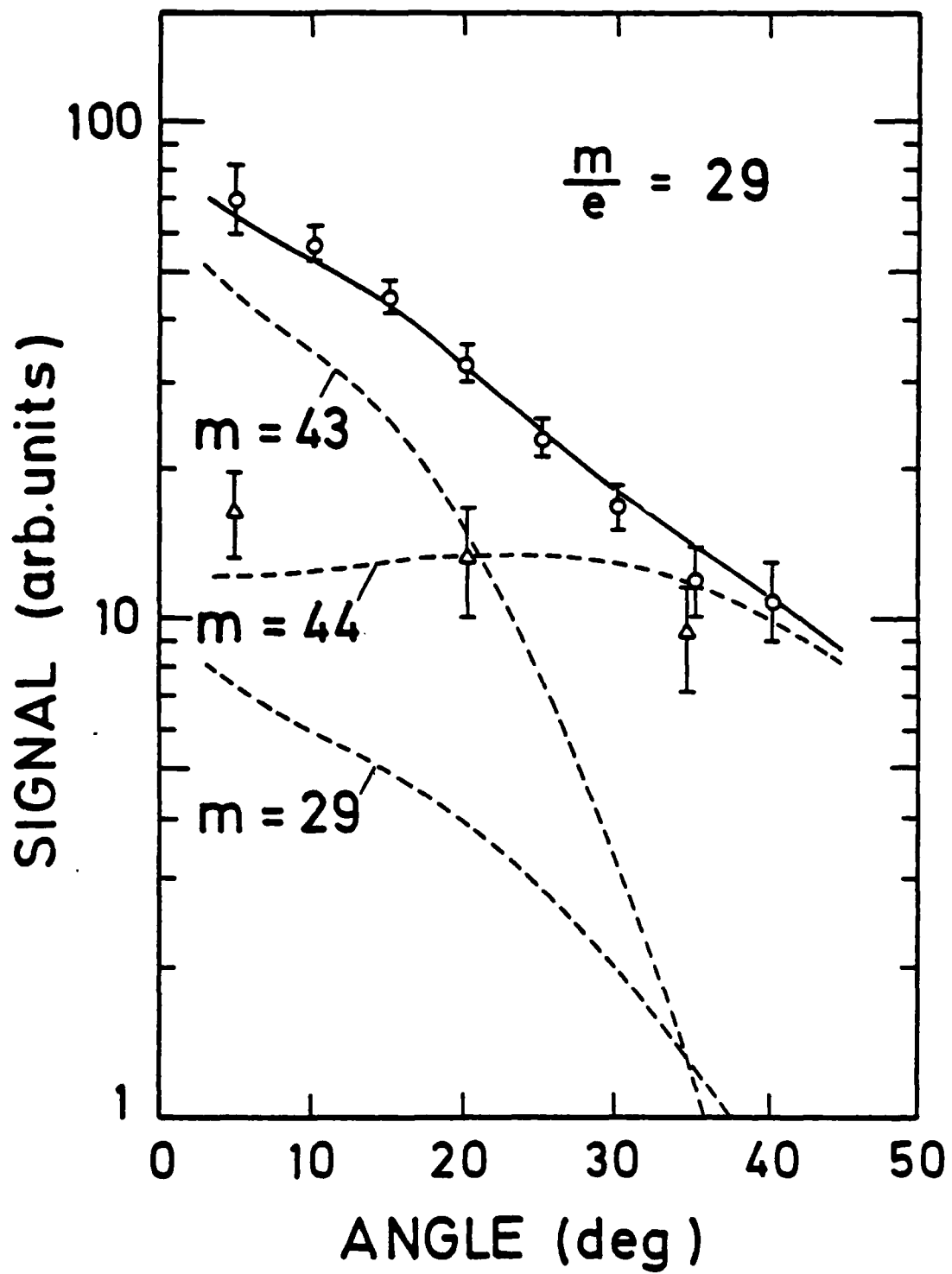


Fig. 10

XBL 8010-12499

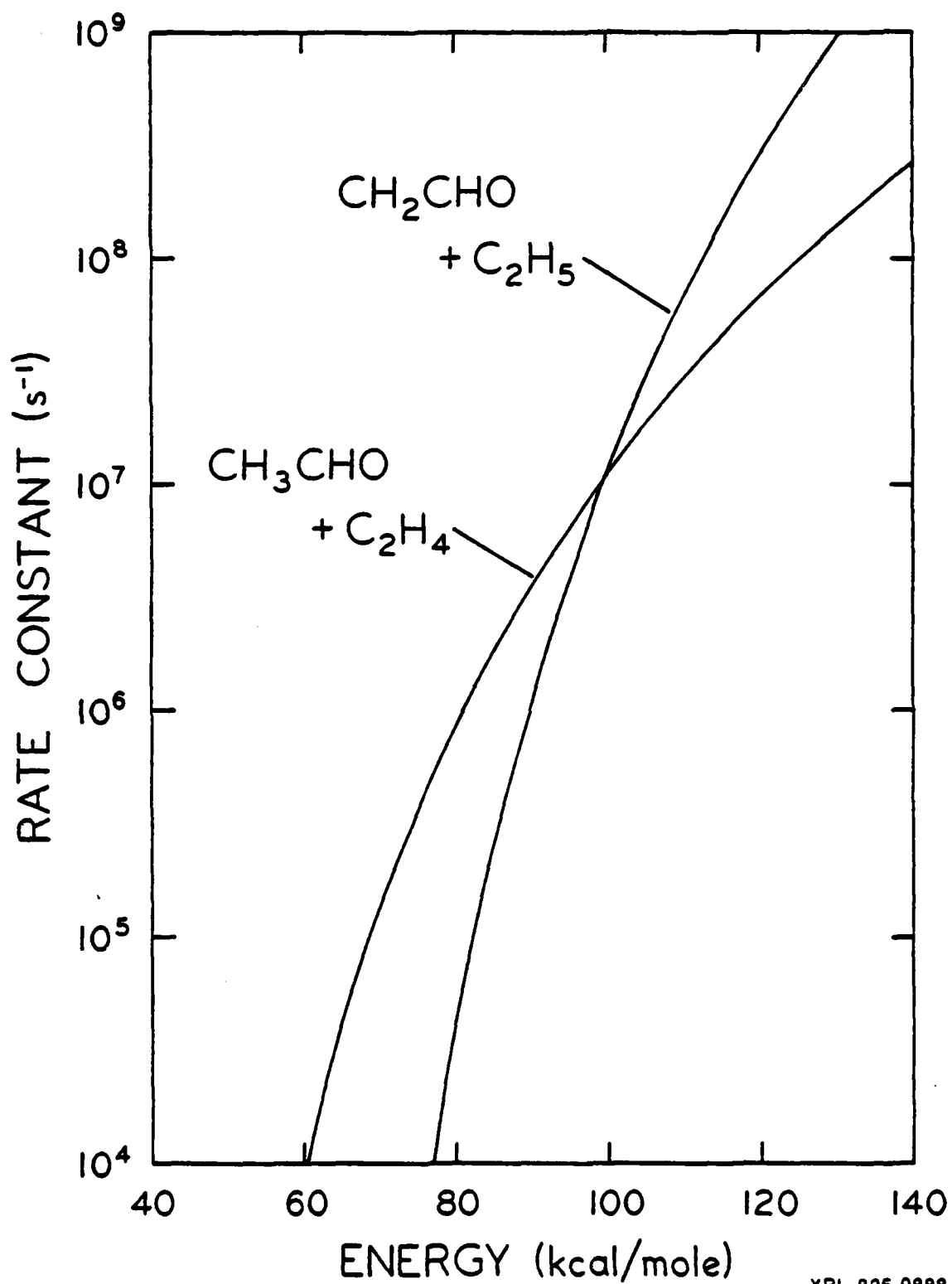


Fig. 11

2. MULTIPHOTON EXCITATION OF DIETHYL ETHER

L. Butler, R. J. Buss, R. Brudzynski and Y. T. Lee

Infrared multiphoton excitation of molecules isolated in a beam has been shown to be a useful tool for studying the dynamics of unimolecular reactions. Most reactions studied by this method have involved simple bond ruptures, isomerization and multicenter elimination of a diatomic molecule. Several studies on larger molecules, ethyl vinyl ether, for example reveal complex mechanisms in which six centered eliminations compete with simple bond ruptures and release an unusually large fraction of available energy as translation.

Pyrolysis studies of diethyl ether¹ have shown two decomposition routes to be dominant: the simple rupture of a C-O bond and the formation of ethanol and ethylene through a four centered cyclic transition state. There has been disagreement concerning the relative rates of these channels.

Using a crossed molecular beam-laser apparatus we have obtained angular and velocity distributions of the products from decomposition of diethyl ether excited by multiphoton absorption from a TEA CO₂ laser. The products were identified by comparing the velocity spectra obtained at various masses and using kinematic relations as well as energy and momentum conservation to distinguish dynamically distinct channels. The time of flight spectrum of mass 45, from the simple bond rupture yielding C₂H₅ + C₂H₅O is shown in Fig. 1. The much faster mass 31 signal, shown in Fig. 2 is identified as arising from the four centered reaction C₂H₄ + C₂H₅OH.

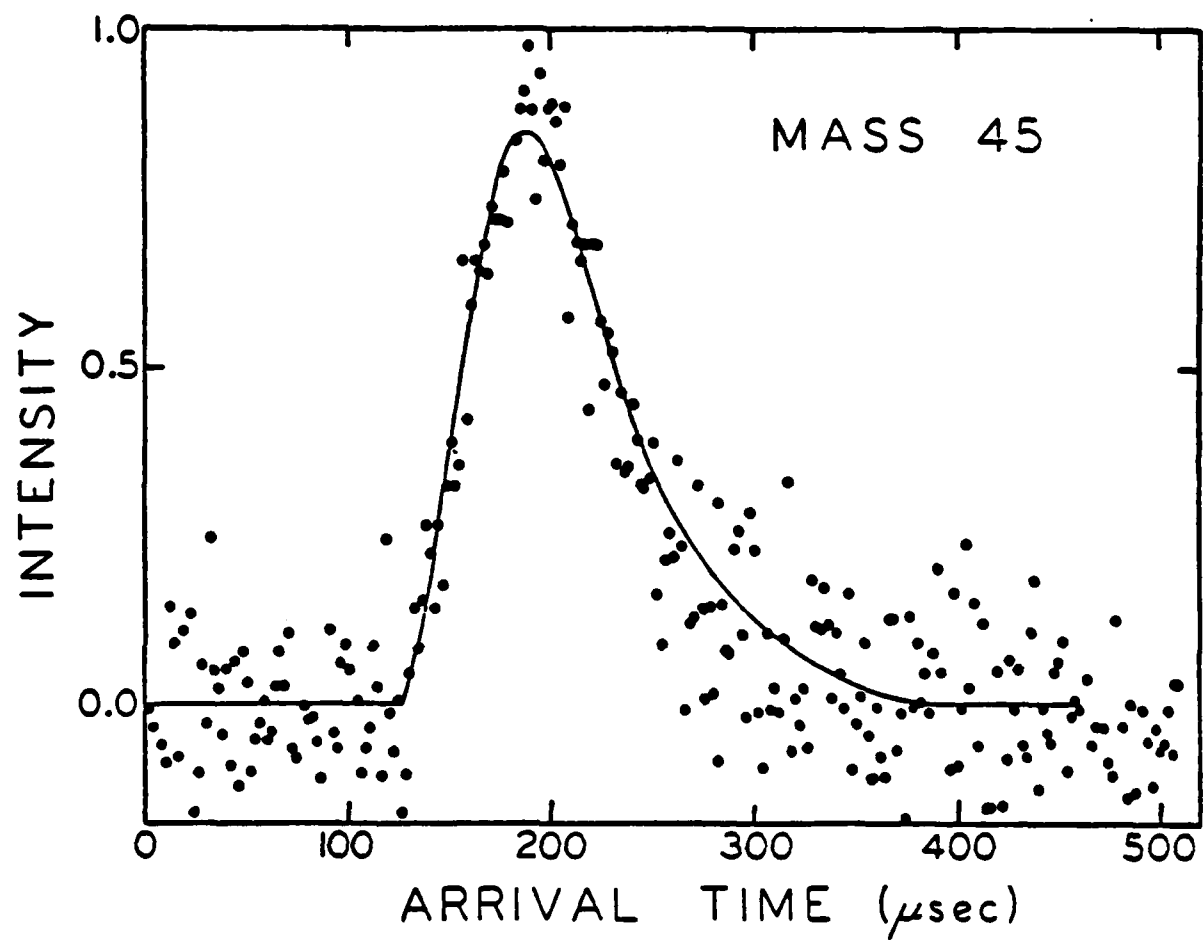
The experimentally determined product translational energy distributions for both channels show that the four centered reaction results in a large

energy release to translation (average ~40%) while the simple bond rupture exhibits very low product translation. The branching ratio for the channels at different laser fluence and the dependence of yield on fluence were used to test the previous reports of activation energies and Arrhenius factors for these reactions.

This work was supported by the Office of Naval Research under Contract No. N00014-75-C-0671.

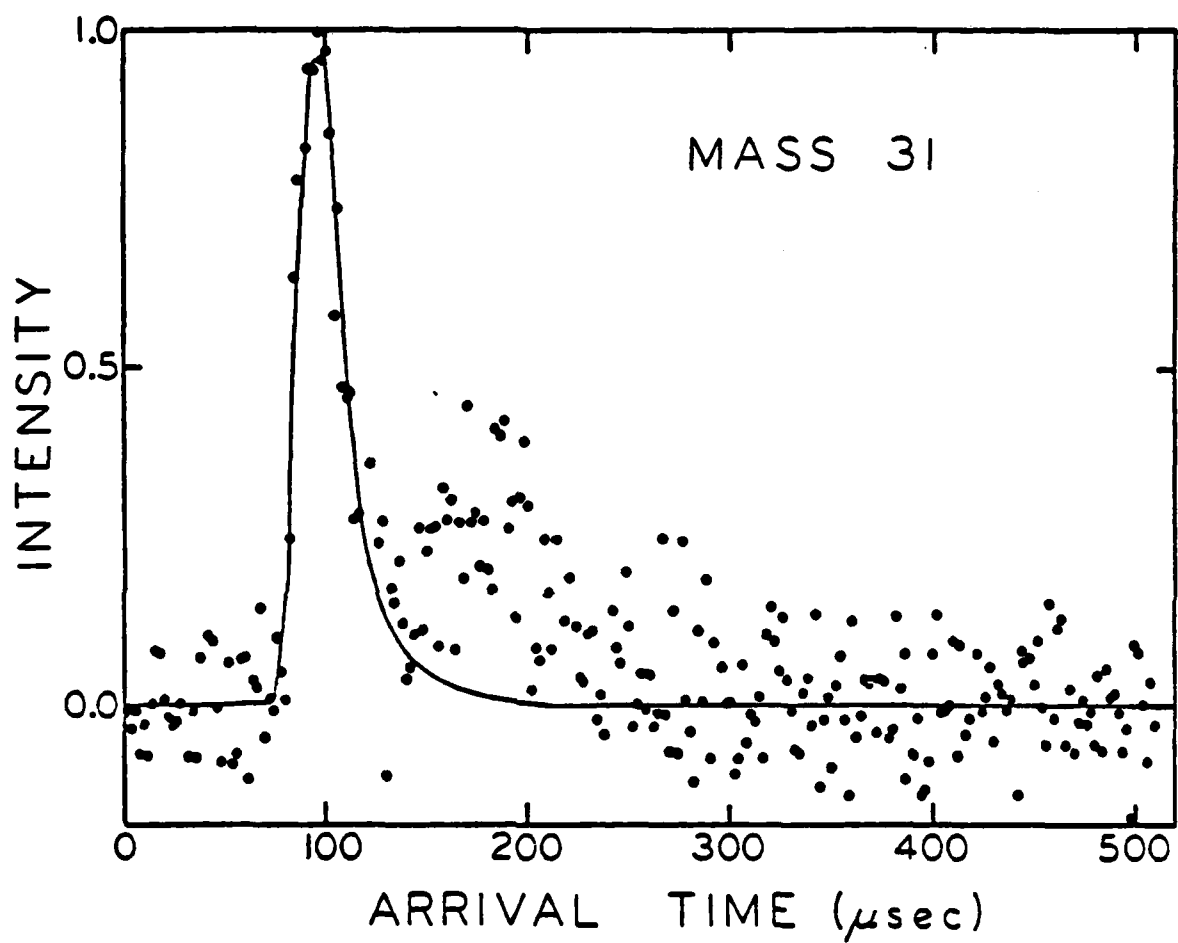
References

1. K. J. Laidler and D. J. McKenney, Proc. Roy. Soc. 278A, (1964) 517.
I. Seres and P. Huhn, Magy. Kem. Foly. 81(3) (1975) 120.



XBL 824-9130

Fig. 1. Time of flight spectrum of product measured at $m/e = 45$, which corresponds to the formation of $C_2H_5 + C_2H_5O$ products.



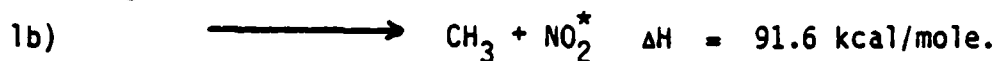
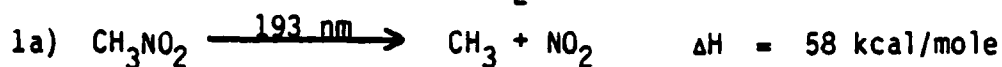
XBL 824-9133

Fig. 2. Time of flight spectrum of product measured at $m/e = 31$, which corresponds to the formation of $\text{C}_2\text{H}_4 + \text{C}_2\text{H}_5\text{OH}$ products.

3. Photodissociation of Nitromethane and Nitroethane

D. J. Krajnovich, L. J. Butler and Y. T. Lee

The nitroalkanes have an intense absorption band around 200 nm which is due to a $\pi \rightarrow \pi^*$ transition on the nitro group. We excited this transition in nitromethane using the ArF excimer at 193 nm. It appears that the only primary dissociative process at this wavelength is the rupture of the C-N bond to produce methyl radicals and NO_2 , but that the NO_2 produced is of two types, vibrationally hot NO_2 and electronically excited NO_2^* :



The NO_2 and CH_3 products were detected with the mass spectrometer at the parent ions, NO_2^+ ($m/e = 46$) and CH_3^+ ($m/e = 15$), respectively.

Time-of-flight (TOF) distributions measured at these masses were correctly related by momentum conservation, but a significant fraction of the slow NO_2 product was not detected. There is strong evidence that this was the result of a secondary dissociation as explained below. The mean combined translational energy of the CH_3 and NO_2 products was 13.5 kcal/mole. Since the energy of an ArF photon corresponds to 148 kcal/mole, there remains, on average, 78 kcal/mole of internal energy (rotational, vibrational, electronic) to be shared between the products.

Besides NO_2^+ and CH_3^+ , signal was observed at NO^+ , O^+ , CH_2^+ and CH^+ in the mass spectrometer. The distributions of CH_2^+ and CH^+ are identical to that of CH_3^+ , indicating that these are all ionizer cracks of the methyl radicals produced in rxn. (1). However, the NO^+ and O^+ TOF distributions are not exactly the same as that of

NO_2^+ . Both the NO^+ and O^+ TOF spectra have a fast shoulder which is absent from the NO_2^+ TOF. Also, this shoulder extends to shorter times in the case of O^+ than in the case of NO^+ . A possible explanation of these results is that some of the NO_2 produced in rxn. (1) is undergoing secondary dissociation to form $\text{NO} + \text{O}$:



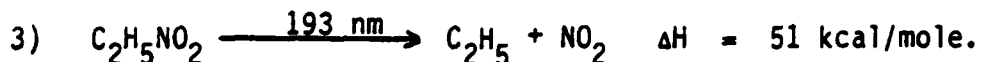
This is further supported by the fact that some of the slow NO_2 product from the primary photodissociation was not detected. The NO product would then contribute the fast shoulder in the NO^+ TOF spectrum, while both NO and the even faster O atom product would create the shoulder in the O^+ TOF spectrum. If this explanation is correct, then the NO^+ and O^+ TOF spectra should exhibit some dependence on the laser power. Specifically, if the shoulder is due to the secondary dissociation rxn. (2), then the shoulder should decrease relative to the main peak as the laser power is decreased. Such an effect has been observed, although the power dependence was much weaker than expected on the basis of the known absorption cross-sections for (room temperature) nitromethane and NO_2 . It appears likely that the NO_2 molecules which undergo secondary dissociation constitute a significant fraction of the total NO_2 yield, and that this fraction, by virtue of its particular internal excitation, has a much higher absorption cross section at 193 nm than vibrationally cold, ground electronic state NO_2 . In any case, more detailed information will be required before this secondary dissociation process can be fully understood.

To gain further information on the nature of the NO_2 product that was lost to the secondary dissociation we analyzed the differences between the

methyl TOF which reflects the primary dissociative process and the NO_2 TOF which contains the NO_2 molecules from the primary process which did not absorb a second photon and dissociate by (2). We were able to conclude that the translational energy distribution of the NO_2 molecules which were lost to the secondary dissociation had a mean combined translational energy of ~ 6 kcal/mole and were all < 16 kcal/mole. These NO_2 molecules could thus be either vibrationally hot ground state molecules from 1a) or electronically excited molecules from 1b) or both. The shape of the subtracted TOF distribution indicated that both contributed to the secondary dissociation products. With less than 84 kcal/mole of internal energy only 3 electronic states of NO_2 are energetically possible, the ground state $X(^2A_1)$ and two electronically excited states $A(^2B_2)$ and $A(^2B_1)$. Dipole selection rules for absorption of a 193 nm photon from these states indicate that only the $X(^2A_1)$ and the $A(^2B_2)$ state would contribute significantly to the secondary dissociation.

Thus, the shape of the methyl TOF indicates that the primary dissociation produces both ground state and electronically excited NO_2 , and the difference between the CH_3 and NO_2 TOF indicates that some fraction of each of the NO_2 products with small translational energy absorbed a second photon and dissociated by (2) causing a faster shoulder to appear in the NO TOF and faster O products to be detected than the primary process alone would explain.

The results for nitroethane photodissociation at 193 nm are quite similar to those for nitromethane. The only primary dissociative process involves C-N bond rupture:



The C_2H_5 and NO_2 were detected as C_2H_5^+ and NO_2^+ , respectively. Concerted reaction to produce ethylene and HONO does not proceed to any measurable extent (no HONO^+ could be detected). As in the case of nitromethane, some secondary dissociation of NO_2 is observed.

There is one interesting difference between the nitromethane and nitroethane photodissociations which is due to the fact that ethyl radicals, unlike methyl radicals, have a low energy unimolecular decomposition channel:



The C-H bond strength is so weak because, as the hydrogen leaves, a C-C double bond is formed simultaneously. Experimentally we observe a

significant difference between the TOF spectra measured at $m/e = 29$

(C_2H_5^+) and $m/e = 26$ (C_2H_2^+), the latter of which may have contributions from

both C_2H_5 and the ethylene formed in rxn. (4). It appears, however, that only a rather small fraction of the ethyl radicals are formed in rxn. (3)

with sufficient vibrational excitation to allow rxn. (4) to proceed.

Spontaneous unimolecular decomposition of radical primary products is

expected to be quite common in the uv photodissociation of larger polyatomic molecules.

4. UNIMOLECULAR DECAY OF TOLUENE

R. J. Buss, D. J. Krajnovich and Y. T. Lee

The dynamics of unimolecular decay processes can now be studied in great detail with the combined techniques of laser preparation of isolated molecules of exact excitation energy in beams and detection of products under collision-free conditions. Of particular interest is the range of applicability of statistical theories in the calculation of specific rate constants and product energy partitioning.

We have investigated the unimolecular decay of toluene in a molecular beam, having prepared the molecule with known excitation energy by the isomerization of cycloheptatriene (CHT) irradiated with a KrF excimer laser at 248 nm. After single photon absorption, CHT is known to undergo rapid internal conversion to the ground electronic state followed by rapid isomerization to toluene. The toluene contains 147 kcal/mole of vibrational energy and might decay by any of several energetically feasible pathways. Previous studies¹ of similarly excited toluene in a gas cell have identified H + benzyl radical products under near collision-free conditions and derived reliable information on the rate of decomposition.

We have observed two primary decomposition reactions yielding H + benzyl radical and CH₃ + phenyl radical, and have obtained angular distributions, shown in the figure, and velocity distributions of the products with a rotatable quadrupole mass spectrometer. The product translational energy distributions for the two channels agreed reasonably well with those calculated by statistical theory. The RRKM calculation was found to somewhat underestimate the high energy product for the H atom elimination. The

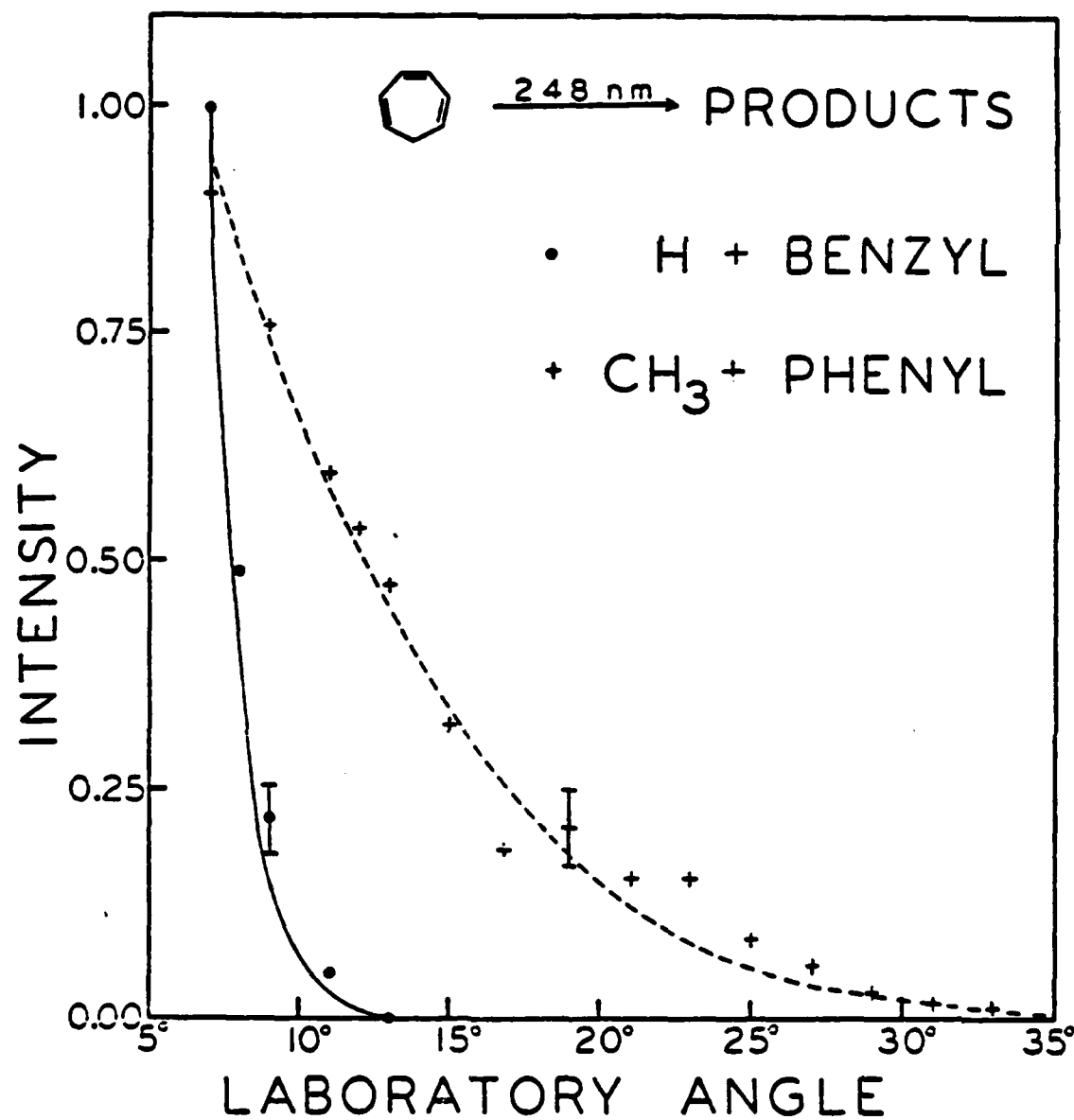
explanation for this deviation may lie in dynamical effects coupling the C-H bending motion to the C-H bond cleavage.

Although it is impossible to accurately determine the relative importance of the H atom and CH_3 radical elimination reactions from our data accumulated so far, it appears that CH_3 elimination is a minor channel of the order of 10% at this excitation energy. A statistical calculation, using reasonable values for the critical configuration parameters, predicts that 2-20% of the excited toluene molecules will dissociate via CH_3 elimination. No evidence for undissociated toluene was observed in experiments with the detector directly viewing the beam, showing that the lifetime of excited molecules is much less than the 0.28 msec flight time to the detector. This is in agreement with the rate constants for unimolecular decay to $\text{H} + \text{benzyl}$ measured by Hippler et al. of $3 \times 10^6 \text{ sec}^{-1}$.

This work was supported by the Office of Naval Research under Contract No. N00014-75-C-0671.

References

1. H. Hippler, V. Schubert, J. Troe and H. J. Wendelken, Chem. Phys. Lett. 84, 253 (1981).



XBL 824-9135

Fig. 1. Angular distributions of products from the KrF laser excitation of cycloheptatriene. Lines are statistical calculations. Typical 1 σ error bars are shown.

II. Publication of ONR Supported Research

A. Papers published or in press

1. On the Photodissociation of Nitromethane at 266 nm. H. S. Kwok, G. Z. He, R. K. Sparks, and Y. T. Lee, *Int. J. Chem. Kinet.* 13, 1125 (1981).

ABSTRACT

In a crossed laser-molecular beam study of nitromethane, it was found that the excitation of nitromethane at 266 nm did not yield dissociation products under collision free conditions. When a small cluster of nitromethane was excited at the same frequency, product was seen only at energies and masses consistent with rupture of the van der Waals bond by vibrational predissociation of the excited state.

2. Methylene Singlet-Triplet Energy Splitting by Molecular Beam Photodissociation of Ketene. Carl C. Hayden, Daniel M. Neumark, Kosuke Shobatake, Randal K. Sparks and Yuan T. Lee. *J. Chem. Phys.* 76, 3607 (1982).

ABSTRACT

The singlet-triplet splitting in methylene has been determined from the measurements of fragment velocities from ketene photodissociation at 351 and 308 nm in a molecular beam. The splitting is found to be 8.5 ± 0.8 kcal/mole. This agrees with many experimental results, but not with the value of 19.5 kcal/mole derived from recent photodetachment experiments on CH_2 .

B. Paper Submitted for Publication

1. Competing Dissociation Channels in the Infrared Multiphoton Decomposition of Ethyl Vinyl Ether. F. Huisken, D. Krajnovich, Z. Zhang, Y. R. Shen and Y. T. Lee. Submitted to *J. Chem. Phys.* (1982).

ABSTRACT

Infrared multiphoton decomposition of ethyl vinyl ether (EVE) has been investigated by the crossed laser-molecular beam technique. Competition is observed between the two lowest-energy dissociation channels: (1) $\text{EVE} \rightarrow \text{CH}_3\text{CHO} + \text{C}_2\text{H}_4$, and (2) $\text{EVE} \rightarrow \text{CH}_2\text{CHO} + \text{C}_2\text{H}_5$. Center-of-mass product translational energy distributions were obtained for both dissociation channels. The products of reactions (1) and (2) are formed with mean translational energies of 31 kcal/mole and 5 kcal/mole,

respectively. The branching ratio shifts dramatically in favor of the higher energy radical producing channel as the laser intensity and energy fluence are increased, in agreement with the qualitative predictions of statistical unimolecular rate theory.

C. Invited Lectures presented during the contract period.

1. Y. T. Lee, "Recent Advances of Photofragmentation Translational Spectroscopy," Western Spectroscopy Association Conference, Asilomar, Pacific Grove, California, January 28-30, 1981.
2. Y. T. Lee, "Dynamics of Infrared Multiphoton Dissociation of Polyatomic Molecules," Lawrence Livermore Laboratory, Livermore, California, March 11, 1981.
3. Y. T. Lee, "Crossed Molecular Beam Studies of Elementary Atomic and Molecular Processes," Lester Kuhn Memorial Lecture, Department of Chemistry, Johns Hopkins University, Baltimore, Maryland, March 17, 1981.
4. Y. T. Lee, "Recent Advances of Molecular Beam Chemistry, Department of Chemistry, Pennsylvania State University, College Station, Pennsylvania, March 19, 1981.
5. Y. T. Lee, "Dynamics of Endothermic Reactions Involving Atoms and Polyatomic Molecules," Debye Award Symposium honoring Professor R. B. Bernstein, American Chemical Society Annual Meeting, Atlanta, Georgia, March 30, 1981.
6. Y. T. Lee, "Energy Splitting Between Singlet and Triplet Methylene," Department of Chemistry, University of Texas, Austin, Texas, April 2, 1981.
7. Y. T. Lee, "Molecular Beam Studies on Reaction Dynamics," Third West Coast Theoretical Chemistry Conference, NASA Ames Research Center, April 22-24, 1981.
8. Y. T. Lee, "Reaction of Oxygen Atoms with Unsaturated Hydrocarbons," Chemistry Department, Tsinghua University, Hsinchu, Taiwan, China, May 26, 1981.
9. Y. T. Lee, "Effect of Vibrational and Translational Energies in Endothermic Reactions," Chemistry Department, Taiwan University, Taipei, Taiwan, China, May 28, 1981.
10. Y. T. Lee, "Photofragmentation Translational Spectroscopy," Academia Sinica, Taiwan, China, May 29, 1981.

11. Y. T. Lee, "Vibrational Predissociation Spectroscopy of Hydrogen Bonded Clusters and van der Waals Molecules," V International Conference on Laser Spectroscopy, Jasper Parks, Canada, June 29-July 3, 1981.
12. Y. T. Lee, "The Current Status of the Reactive Scattering Experiment," XII International Conference on the Physics of Electronic and Atomic Collisions, Gatlinburg, Tennessee, July 15-21, 1981.
13. Y. T. Lee, "Current Status of Reactive Scattering," Gordon Research Conference on "Dynamics of Molecular Collisions" at Plymouth, New Hampshire, July 27-31, 1981.
14. Y. T. Lee, "The Effect of Vibrational Excitation in Ion-Molecule Reactions," 28th International Union of Pure and Applied Chemistry Congress, Vancouver, Canada, August 17-22, 1981.
15. Y. T. Lee, "Reactions of Oxygen Atoms with Ethylene and Vinylbromide," X International Conference on Photochemistry, The University of Crete, Iraklion, Crete, Greece, September 9-12, 1981.
16. Y. T. Lee, "Molecular Beam Studies of Biomolecular Reactions: $F + H_2$ and $Li + HF$," 50 Years Dynamics of Chemical Reactions Conference, Berlin, West Germany, October 12-15, 1981.
17. Y. T. Lee, "Vibrational and Translational Energy Dependence in Reactions of H_2^+ ," American Chemical Society Meeting, Las Vegas, Nevada, March 30-April 1, 1982.